CHEMICAL BATH DEPOSITION AND CHARACTERISATION OF $CdAl_2SO_3$ QUATERNARY THIN FILMS

BY

EZIHE, JAMES A. (B. Tech., FUTO)

(20164027878)

A THESIS SUBMITTED TO THE POST GRADUATE SCHOOL,

IN PARTIAL FULFILMENT OF THE REQUIREMENTS FOR THE AWARD OF THE DEGREE OF MASTER OF SCIENCE (M.Sc.) IN

SOLAR ENERGY PHYSICS

AUGUST, 2019

CERTIFICATION

This is to certify that this work "Chemical Bath Deposition and Characterization of $CdAl_2SO_3$ Quaternary Thin Films'' was carried out by I, Ezihe James A. (Reg. No. 20164027878) in partial fulfillment for the award of the degree of M.Sc. in Solar Energy Physics in the Department of Physics, Federal University of Technology, Owerri.

.....	17/02/2020
Prof. D. D. O. Eya (Supervisor)	Date
.....	17.02.2020
Dr. C. Iroegbu (Co-Supervisor)	Date
.....	17/2/2020
Prof. (Mrs.) C. A. Madu (Head of Department)	Date
.....	18/2/2020
Prof. C. C. Z. Akaolisa (Dean School of Physical Sciences)	Date
.....	.....
Prof. (Mrs.) N. N. Oti (Dean Post Graduate School)	Date
.....	04/02/2020
Prof. B. A. Ezekoye (External Supervisor)	Date

DEDICATION

I dedicate this work to my mother, Mrs. Lauretta C. Ezihe.

ACKNOWLEDGEMENTS

My sincere appreciation and gratitude go to my research supervisor, Prof. D. D. O. Eya and co-supervisor Dr. C. Iroegbu who continuously guided and supervised me throughout my research work. My deepest gratitude goes to Dr. O. K. Echendu and Mr. K. Egbo whose tireless efforts saw me through the characterization stage of my work.

I also recognize, the post graduate co-ordinator, Dr. K. B. Okeoma for his moral support. I will not fail to appreciate, Head, department of Physics. Prof. Mrs. C. A. Madu for her motherly support. My special thanks go to the vice chancellor of the Federal University of Technology, Owerri, Prof. Francis C. Eze, for his care and support.

I also extend my heartfelt thanks to Mr. Ogundeji, O. Samuel who regularly assisted me throughout the experimental stage of my work. I also appreciate the lab. technologist and lab assistant Mr. Orame E. and Mr. Linus, I. Chidi respectively for their help during the preliminary stage of the characterization.

My special thanks go to all staff of the Department of Physics, Federal University of Technology, Owerri for their contribution in the research work.

TABLE OF CONTENT

LIST OF TABLES

LIST OF FIGURES

LIST OF PLATES

ABSTRACT

Quaternary cadmium aluminiumsulphite ($CdAl_2SO_3$) thin film were synthesized via chemical bath deposition (CBD) technique using a reaction bath containing cadmium chloride, thiourea, and Aluminiumsulphateoctadecahydrate at room temperature. The thin films are white in colour and strongly adherent to the substrate. The materials were annealed at various temperatures of 150 °C, 200 °C and 250 °C before characterizing, using glancing incident X-Ray diffraction (GIXRD) and Raman spectroscopy for structural analysis, UV-Vis-NIR spectrophotometer for optical analysis, Energy Dispersive X-Ray(EDX) spectroscopy for compositional analysis, 3D thickness profiling for thickness of the films and Scanning electron microscopy (SEM) for morphological analysis. The XRD results showed that the $CdAl_2SO_3$thin films crystallize as binary-phase compounds of $CdSO_3$ and Al_2O_3. The optical measurements show that the films have low transmittance in the photon wavelength of 300-900 nm explored. The films have very high absorbance across the wavelengths under study, with the highest absorbance of 99.5 % in the UV region of the solar spectrum. The $CdAl_2SO_3$ real dielectric constant value is of the range of 1.5 to 1.9, and the imaginary dielectric constant has the range of 1.5 to 2.28. The direct bandgap of the $CdAl_2SO_3$ thin films ranges from 3.75 eV to 4.10 eV. The thickness of the material ranges 207 nm to 879 nm. The SEM micrographs reveal homogenous and densely packed grains. The rough estimate of the grain size ranges from 15µm to 70µm. The EDX spectra reveal the presence of Cd, Al, S and O in the films investigated. The high absorption in the UV-Vis regions makes the material suitable for thin films absorber solar cells. The direct bandgap of the thin films makes them applicable in optical devices such as LEDs and semiconductor lasers.

Key words: $CdAl_2SO_3$, thin films, bandgap energy, absorbance.

CHAPTER ONE

INTRODUCTION

1.1 Background Information

A thin layers (less than about 1 micron) crystallite or non crystallite material grown on a substrate by wet or dry method is known as thin films. Thin films are important because of the minimal usage of materials and have the potential of reducing the material cost while still maintaining the standard of application. Imperatively, thin films can help reduce cost for materials that are expensive. Minimal weight requirement is another important parameter for thin films application.

Thin films play pertinent role in almost all optoelectronic and photonic devices. 'They are being used as electroplating films for decoration and protection' (Heaven, 1970). 'Thin films are used as anti-reflection coatings on window glass, video screens, camera lenses and other optical devices, these films are less than 100 nm thick, made from dielectric transparent materials and have refractive indices less than that of the substrate' (Penti *et al.*, 2004).

One of the important techniques researchers are interested in is the chemical bath technique because of the inexpensive mode of its operation. Many materials have been produced through this technique. 'Among these materials that are of great interest include metal chalcogenides especially binary (2) elements such as CdS and PbS from group II and group VI elements doping them through CBD has been done to make them suitable for use as window layers using different elemental dopants like boron' (Khallaf*et al.*, 2009), 'indium' (Shadia*et al.*, 2008), 'arsenide and chlorine' (Amanullah*et al.*, 2005).

According to (Mosiori, 2012) ‘Ternary derivatives of CdS have generated a lot of research interest because of their varied applications in the field of optoelectronic devices’.

1.2 Problem statement

In view of high cost of solar cells/panels, it is pertinent to study and scout for good, cost effective materials for solar cell fabrication that efficiently convert solar energy to electrical energy. Thin film reduces the amount of material used to a minimal level and hence raises high prospect for cost effectiveness. The deposition and characterization of cadmium aluminium sulphite thin films is geared towards achieving cost effective material for solar energy and other electronic applications.

1.3 Objectives of Study

To grow and characterize cadmium aluminium sulphite thin film material for thin film solar cell production and other possible applications is the aim of this work.

The specific objectives of this study are to:

a. deposit thin films of $CdAl_2SO_3$ by CBD technique.
b. characterize the thin film to determine their structural, compositional, morphological, optical and solid state properties.
c. determine the influence of thermal treatment on the structural, optical, morphological and compositional properties of the material.
d. analyse these properties for possible applications in thin films solar cells and optoelectronic devices.

1.4 Justification of Study

Owing to the fact that silicon solar panels especially the bulk wafer are expensive and difficult to produce, there is need to manufacture thin film materials that are cost effective. $CdAl_2SO_3$is a potential direct bandgap semiconductor material with efficient optical properties for solar energy conversion. When successfully deposited using very cost effective technique, chemical bath deposition technique, and characterized, the thin film material could be a veritable asset for bringing down unit cost of solar cells.

1.5 Scope of Study

This research work, is limited to the growth of nanocrystallite $CdAl_2SO_3$ thin films on glass substrates using CBD techniques and characterize them. The influences of thermal treatment on the compositional, structural, morphological and optical properties of the material were also investigated.

CHAPTER TWO

LITERATURE REVIEW

2.1 Ternary Thin Films

Ternary semiconductors are three elements in one compound semiconductor. 'Ternary chlcogenides are now very important area of interest for researchers of thin films, because they have great potential for applications in solar cells, light emitting diodes and non – linear optical devices' (Ortega *et al.*, 2003). 'Ternary compounds are found to be promising materials for optoelectronic device applications such as green emitting devices and are also suggested to be possible materials for window layer of solar cells' (Woon – Jo *et al.*, 2003). 'The optical and solid state properties of ternary chalcogenide thin films of $AgAlS_2$ make them potential semiconductor materials for electronic applications' (Okoli*et al.*, 2006). Various growth techniques had been employed in ternary chalcogenides thin films deposition, Uhuegbu (2011) deposited FeZnS and Mohammed *et al.* (2009) deposited PbCdS thin films by chemical bath method, Noriyuki *et al* (2013) deposited CuZnS and Ortega *et al.* (2003) deposited AgInS2 thin films by spray pyrolysis. Sunyoung*et al.* (2008) deposited CdZnSe thin films by photo electrochemical method.

Quaternary thin films are four elements in one compound semiconductor. Quaternary compound of Cu_2FeSnS_4 (CFTS) thin films a potential absorber layer had been reported by different authors Xiaoohui *et al*. (2017) and Haijun*et al*. (2017) produced by electrochemical deposition method and solvothermal method respectively. Also Lei Meng *et al*. (2015) reported quaternary thin films of Cu_2CdSnS_4, while Xie-Min *et al*. (2013) reported Cu_2ZnSnS_4 quaternary thin films.

2.2Methods of Thin Films Deposition

Thin film deposition is the process of growing thin films on the surface of a substrate. These films are in the range of nanometer to micrometer in thickness. There are many ways of preparing chalcogenide thin films. The techniques range from very simple and cheap to complex and very expensive ones depending on the substrate, coating materials and on the required performance of the thin films (Quijada*et al.*, 1998; Chopra, 1969).

In thin film deposition, three basic steps are followed in the formation of the films. These steps are: creation of the species required for film formation, the transport of these species through a medium, and the condensation of the species on the substrate and subsequent coalescence to form the film'. (Chopra, 1969)

The methods for depositing thin films may be broadly categories into two headings: physical and chemical techniques.

2.3 The Physical Deposition Techniques

This technique makes use of thermodynamics, electromechanical and mechanical means to produce a thin film of material. Films deposited by this method are usually directional. Some of the examples of this method include: molecular beam epitaxy, laser beam evaporation, sputtering, physical vapour deposition (PVD), plasma techniques, thermal evaporation, electron beam evaporation, arc evaporation, ion plating evaporation, etc (Maissel *et al.*, 1970).

2.3.1 Thermal Evaporation

Thermal evaporation is the method where by substances used as films are thermally vaporized and then deposit on substrate due to difference in potential with little or no collision with gas molecules.

According to (Gunder, 1966; Young*et al.*, 2002). 'Deposition rate and thickness can be controlled by various systems: (i) by making use of quartz crystal that changes frequently with change in film thickness on the face of the substrate, (ii) by the use of ionization gauge- this measures the excess ion current due to the presence of the evaporant, (iii) by employing mechanical arrangement that deflects due to impingement of the vapour species or as a result of the weight of the film'. Two or more sources give rise to multi-phase films. 'The establishment of equilibrium is prevented in convectional thermal evaporation because the vapour is removed immediately from the vicinity of the molten source, this leads to elements with the highest vapour present in the source alloy, to evaporate first thereby depleting the source and leading to compositional in-homogeneities in the deposited film. In order to remedy the situation, use is made of flash evaporation' (Kijatkina*et al.*, 2003, Lee*et al.*, 2003, Coutts, 2002). 'In flash evaporation, powdered material is dropped steadily onto a heated ribbon, thereby almost instantaneously evaporating it. A further complication may arise in both flash and convectional evaporation that the dominant (equilibrium) vapour species may not have the same composition as the source material' (Coutts, 2002).

'Apart from the resistive' (Pawar*et al.*, 1986, Huang*et al.*, 1982) 'and radio frequency heating' (Ibrahim, 1995) techniques, there are other methods of vacuum evaporation which is dependent on the nature of the evaporant. 'These include arc evaporation which is mainly for refractory metals such as W, Nb, Ta and Mo'(Bhattacharya*et al.*, 1983 ; Rai, 1993), 'exploding wire technique' (Raghupathi*et al.*, 2005, Rodrigo*et al.*, 2002) 'and laser evaporation' (Nair*et al.*, 1987).

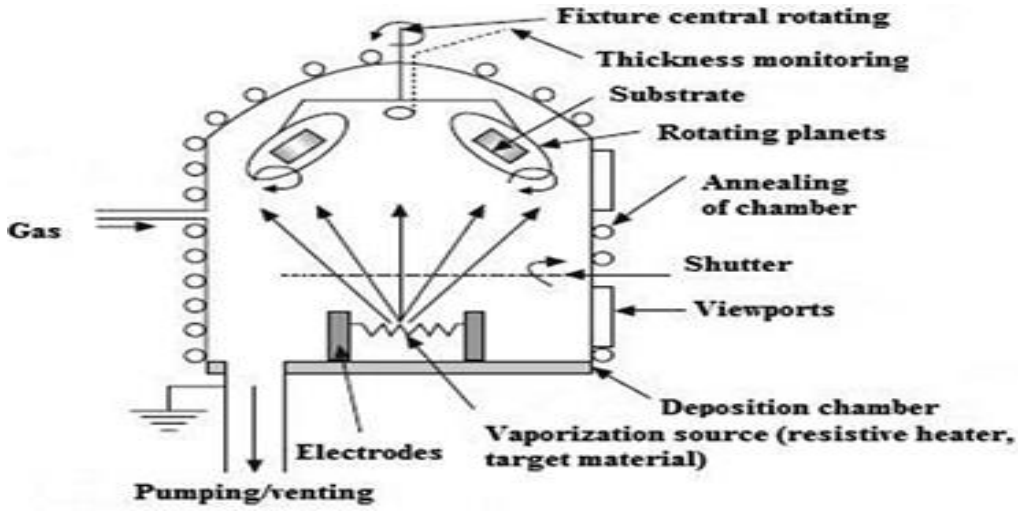

Fig., 2.1: Schematic diagram for Thermal Evaporation(Asim *et al.*, 2017)

2.3.2 Sputtering Deposition

Sputtering is one of the ways of depositing films via sputter deposition. 'It consists basically of the bombardment of a target by emergent ions from a low pressure plasma causing erosion of material either atom-by-atom or as cluster of atoms and subsequent deposition of a film on a substrate' according to (Maissel, 1966; CruzVazquez*et al.*, 2001).

Sputtering is significantly better than evaporation for the production of multi-phased compounds. This is due to the fact that sputtering rate for different elements does not vary significantly, like evaporation rate, vapour pressure, and melting points.

'As a consequence sputtered films tend to preserve the stoichiometry of the starting material, sputtered SiO_2 is an example' (Maissel*et al.*, 1970). The schematic diagram for sputtering is given in figure 2 below.

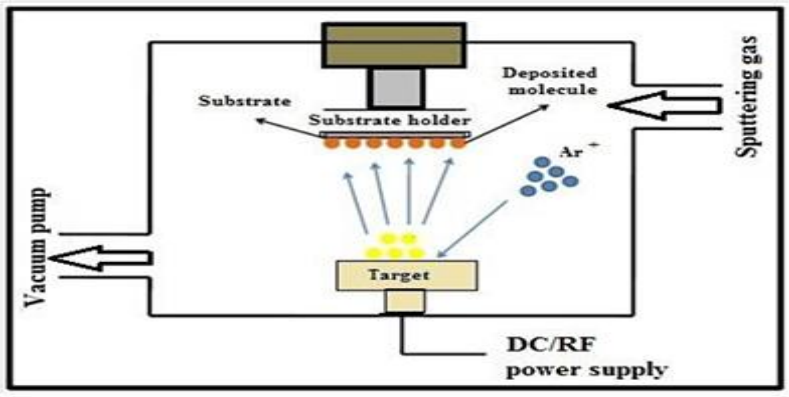

Fig., 2.2: Schematic diagram for sputtering (Asim*et al.*, 2017)

2.3.3 Epitaxial Deposition

The growth of a mono crystal film on crystallite substrate is known as epitaxial growth. Oriented films growth can be achieved by epitaxial process. If the film formed is of the same material as the substrate we have homoepitaxy but different material from the substrate gives heteroepitaxy.

Epitaxial temperature depends on the rate of the evaporation for a given pair of material. R which is the deposition rate is denoted by

$$R = Aexp\left(\frac{Q_d}{k_\beta T_e}\right) \qquad 2.1$$

Where A is a constant, the epitaxial temperature is given by T_e, the activation energy is Q_d, and Boltzmann constant is k_β. Epitaxy is formed at lower deposition rates but at higher rates crystal twins are formed. The epitaxial growth techniques are complex, very expensive and undesirable for large scale production. The technique is reserved only for studies that require special applications. Techniques involved in epitaxial method include: molecular beam epitaxy (MBE), solid phase epitaxy (SPE), hot wall epitaxy (HWE), liquid phase epitaxy (LPE) etc.

2.3.4 Molecular Beam Epitaxy (MBE)

The epitaxial method for thin films deposition in an ultra high vacuum system for a single crystal from an effusive source is known as molecular beam epitaxy. MBE method is required for epitaxial growth of great purity and also of good crystal structure. MBE is one of the major techniques used in nanotechnologies, semiconductor devices and optoelectronic industries.

'Several advantages are offered by MBE to the silicon device industry. The first is the capability of growing new structure which cannot otherwise be fabricated. The second is improved dopant control. The third is that new material combinations are possible with a low growth temperature and a high purity ultra high vacuum environment' (Uhuegbu, 2007).

2.4 The Chemical Deposition Techniques

In this method, a solid layer is formed on the substrate by chemical changes of the precursors. The films of this technique are not directional as in the case of physical techniques but conformal. This method has the advantage of being simple and cost effective. Some of the examples of this method include: chemical vapour deposition (CVD),sol-gel technique, spin coating, Electroplating technique, chemical bath deposition (CBD), Spray pyrolysis technique, Electrolysis deposition, electrochemical deposition (ECD), anodization, dip coating, etc.

2.4.1 Electrochemical Deposition (ECD)

The deposition of films or metal thin coatings on conductive substrate by electrolysis from solution containing the desired metal ions is known as

electrochemical deposition. The process is governed by the two Faraday laws of electrolysis:

i. the quantity of electricity passed is directly proportional to the quantity of electricity passed.

ii. the masses of the different substances dissolved or deposited at the electrodes by the passage of a given amount of electricity are equivalent to the time or chemical equivalent weights. The summary of the two laws is given by the relation.

$$m = \frac{IEt}{F} \qquad 2.2$$

Where m is the mass in grams of the substance deposited when a current I (in ampere, A) is passed for a time, t (in seconds, s). E is the chemical equivalent weight in grams of substance deposited and F is the Faraday constant given as 96,500 coulombs. The constant is the quantity of charge required to deposit one equivalent weight of any ion from solution. The deposition bath consists mainly of electrolyte that provides ion required for deposition. On dipping a metallic electrode in the solution, a dynamic equilibrium of the form below is achieved.

$$M \leftrightarrow M^{n+} + ne \qquad 2.3$$

Where M represents the atom ofthe metal, n the level of ionization and e the electronic charge. In the absence of an external applied field therefore, there is a resultant potential between the electrodes and the electrolyte. This potential is known as the electrode potential. This is known as the electrical double layer. External electric field is usually applied during electrochemical drift to the electrode where the necessary electrochemical reaction takes place resulting in the deposition of the desired material. Concentration gradient is always created in the region because of the rapid depletion of the ions from the double layer. However, this is compensated by a continuous drift of ions to the electrode from the bulk of

the electrolyte. Electrochemical deposition techniques are affected by factors like the pH of the electrolyte, current density, bath temperature and composition, electrode slope and agitation. 'The technique has been used in depositing metal films like Cu, Ag, Au, etc; alloy films like Cu-Sn, Co-Ni, etc. and semi-conducting films on conducting substrates' (Chopra and Das, *1983;* Echendu*et al.*,2014; Echendu, 2014).

2.4.2Anodization

The electrochemical way of turning metal surfaces into corrosion resistant, durable, decorative finish is known as anodization. In this technique, the metal to be coated is made the anode in the electrolyte solution containing its metallic ion. When electric current is passed via the solution the anode is coated with ions of its compound. The technique is mainly for forming oxide films on the surface of a metal. Films thickness is directly proportional to the applied voltage for specific period of time. The thickness of layer grown per unit voltage is called anodization constant which varies for different metals.

2.4.3 Chemical Vapour Deposition (CVD)

The condensation of compound(s) from gaseous phase onto a substrate is called CVD. Sometimes external means can be used to activate the chemical reaction. These include the heat or electron bombardment, application of an electric arc or glow discharge, light or x-rays etc. The nature of chemical reaction in CVD techniques could be grouped as: Disproportionation, thermal decomposition, chemical transport reactions, nitridation, hydrogen reduction, carbidization, oxidation, or combination of the above.

2.4.4Cathodic Deposition

This is another form of electroplating. ‘Two metal electrodes are dipped into an electrolyte solution and on application of an external field across the electrodes, metal ions from the solution are deposited on cathode as a film, deposition of the films is controlled mainly by the electrical parameters such as, electrode potential and current density’ (Echendu, 2014).

2.4.5 Liquid Phase Epitaxy

Semiconducting epitaxial films are deposited by liquid phase epitaxy (LPE) growth based on crystallization of semiconducting materials dissolved in a suitable metal. ‘Metals of low melting points (e.g. Sn, In, Pb, Bi, Ga) are better suited for this. If a saturated solution ofthe working materials is prepared at high temperature ($\sim 1000°C$) and gradually cooled, the solution becomes supersaturated and crystalline phase begins to grow over a given substrate, growth of quality films of group III-V compounds have been prepared by the LPE technique’ (Chopra *et al.*, 1983).

2.4.6 Sol-gel

Oxide materials synthesis can be achieved via sol-gel technique. This method yield good homogeneity for multi-component materials, and works well under low temperature. The word ‘sol’ stand for production of a colloidal suspension and ‘gel’ denotes the conversion of ‘sol’ to viscous gel or solid materials.

‘Sol-gel dip coating requires considerable less equipment and is less expensive when compared with conventional thin film forming processes such as CVD, evaporation or sputtering. Several authors’ (Kushwaha*et al.*, 2005;Scriven*et al.*, 1988; Estrella *et al.*, 2003).

2.4.7 Chemical Bath Deposition (CBD) Technique

This technique is at times called solution growth method. Metal oxide as well as chalcogenides films are mainly produced by this technique. Low temperature is favourable for this CBD technique. The bath solution precursor is comlexed by comlexing agents such as triethanolamine (TEA), ethylene-tetraacetic acid (EDTA) which react with metallic ions to give the complex solution. Sulphur is gotten by the addition of anions such as thiosulphate, thiorea, thioacetamide etc. when the required bath solution is gotten by the complexing agents, the substrates are then inserted vertically into the solution bath at temperatures which vary from room temperature to about 100 ° C according to the desire of the researcher. Annealing is carried out after deposition to enhance the properties of the films material.

This deposition technique has more advantages over the more advanced techniques like the Spray Pyrolysis, chemical vapour deposition (CVD), MBE, Sputtering etc. 'In this technique it is possible to control the film thickness and composition by varying the solution pH, temperature and concentration of the reagents. The ability of CBD to coat large areas in a reproducible and low cost process is one added attraction of this method. The technique has been used extensively for the deposition of thin films of sulphides and selenides' (Eze and Okeke, 1997; Ndukwe, 1992).

2.5 Optical and Solid State Properties of Thin Film

The solid state and optical properties investigated in this research include: Optical conductivity (σ_o), bandgap Energy (E_g), Transmittance (T), Absorbance (A), Reflectance (R), Absorption coefficient (α), Optical density ($O.D$), extinction coefficient (k), refractive index (n) , the dielectric constants,

2.5.1 Transmittance

According to (Wooten, 1972, Pankove, 1971, Lothian, 1958) . 'The transmittance (T) of a thin film specimen is defined as the ratio of the transmitted flux (I_t) to the incident flux (I_o)' that is,

$$T = \frac{I_t}{I_o} \qquad 2.4$$

'The portion internally reflected eventually comes out considerably attenuated. The end result is that overall transmission is given by' (Wooten, 1972, Pankove, 1971, Lothian, 1958) as:

$$T = \frac{I_t}{I_o} = \frac{(1-R)^2 \exp(-\alpha d)}{(1-R^2)\exp(-2\alpha d)} \qquad 2.5$$

The effect of multiple reflections is governed by equation 2.14. 'When the product αd is large, the second term in the denominator becomes negligible and the transmittance is expressed' as (Lothian,1958)

$$T = \frac{I_t}{I_o} = (1-R)^2 \exp(\alpha d) \qquad 2.6$$

2.5.2 Absorbance

The fraction of radiation absorbed when an electromagnetic radiation strikes the surface of a material is called absorbance (A), it is also expressed as the log to base 10 of transmittance.

$$A = log_{10} {}^{I_t}/_{I_o} = log_{10} T \qquad 2.7$$

Equation 2.17 shows that the transmittance and absorbance are related. In this work transmittance and reflectance data were gotten from the UV-Vis-NIR photo-spectrometer thin film optical measurement. The absorbance was calculated from equation 2.18. The other properties are gotten from calculations based on these quantities (transmittance, reflectance and absorbance).

2.5.3 Reflectance (R)

Reflectance is part of the radiation that is reflected when incident on a surface. By law of energy conservation, absorbance (A), reflectance (R), and transmittance (T), are related by

$$A + T + R = 1 \qquad 2.8$$

2.5.4 Absorption Coefficient (α)

The decrease in intensity when photons impinge a material medium is known as absorption coefficient. It shows the distance light can travel into a material before it is absorbed. 'When radiation of intensity I_o is incident on material of thickness d (μm) the transmitted intensity I_t is given by' (Pankove, 1971, Lothian, 1958) as:

$$I_t = I_0 \exp(-\propto d) \qquad 2.9$$

Equation 2.19 can be expressed as, $T = \frac{I_t}{I_o} = \exp(-\propto$

$d)$ 2.10

$$and \propto = -\frac{[InT]}{d} \qquad 2.11$$

Where the film thickness is denoted by d

2.5.5 Optical Density

The logarithm to base ten of the inverse of transmittance is known as the optical density.

$$Optical\ density\ (O.D) = log_{10}\,{}^{1}/_{T} = log_{10}\,{}^{I_o}/_{I_t} \qquad 2.12$$

2.5.6 Band Gap Energy (E_g)

The energy required to move an electron into the conduction band from the valence band is the band gap energy. It is the minimum energy required to excite an electron into the conduction band. Hole is created in the valence band when an electron is excited into the conduction band. 'When an electron undergoes transitions from an upper part of the valence band to the lower part of the conduction band, it causes dispersion near the fundamental absorption edge and gives the shape of the absorption spectrum'. (Macmanon, 2002). 'The relation between the absorption coefficient, α, and the incident photon is' (Eze and Okeke, 1997; Ndukwe, 1992);

$$(\propto h\nu)^n = A\left(h\nu - E_g\right) \qquad 2.13$$

Where $E_g$is energy bandgap, A is constant, and n is an index which can take the values of *2, 1/2*, *2/3*, and *1/3* in accordance with the electronic transition.

A common method for determining band gap values for deposited films is by making plots of $(\propto h\nu)^n$versus hν. 'The extrapolation of the straight portion of the plot onto the hv axis gives the band gap energy, $E_g$of the material. For direct gap transition, *n = 2*, and for indirect gap transition, *n = ½*' (Chao, 2011).

'The size of the band gap determines the area of application of the material, thin films with narrow gaps are used basically as solar absorber materials for solar cell

fabrications and large selective coatings for photo-thermal conversion of solar energy, thin films with wide gap can be used in production of LEDs, photodiodes, sensors for gas detectors, electrode and piezoelectric devices, varistors and optoelectronic devices' (Ezekoye*et al.*, 2013).

2.5.7 Refractive Index (n)

The behavior of light when it propagates from one medium to another can be described by refractive index. It shows the amount of light bend when it travels through a material. 'The refractive index determines the propagation speed (v) of light in the material medium according to the relation $n=c/v^2$', (Echendu *et al*, 2014) , where v is the speed in the medium and c is the speed of light. 'The boundary between vacuum and an absorbing layer specified by refractive index (n) and the extinction coefficient (k) at normal incidence, yields the reflectance in terms of optical constants of the layer by' (Coutts, *et al.*, 2001; Mahrov, *et al.*, 2004) as

$$R = \frac{(n-1)^2 + k^2}{(n+1)^2 + k^2} \qquad 2.14$$

'For semiconductors and insulators, or materials in the range of frequencies in which absorption is weak, $k \ll (n-1)^2$so that $equation$ 2.26 becomes' (Coutts, *et al.*, 2001; Mahrov, *et al.*, 2004)

$$R = \frac{(n-1)^2}{(n+1)^2} \qquad 2.15$$

Thus

$$n = \frac{1 + \sqrt{R}}{(1 - \sqrt{\mathrm{R}})} \qquad 2.16$$

Thus, to find n for any particular wavelength, the reflectance is calculated first then the refractive index, *n*.

2.5.8 Extinction Coefficient (k)

This is a measure of depth of penetration of radiation with respect to absorption. It refers to several diffraction measures of the absorption of light in a medium. 'The absorption coefficient (α) can be defined with reference to extinction coefficient (k) as' (Coutts *et al.*, 2001; Mahrov*et al.*, 2004)

$$\propto = \frac{4\pi k}{\lambda} \qquad 2.17$$

$$k = \frac{\alpha\lambda}{4\pi} \qquad 2.18$$

Where k is the extinction coefficient.

2.5.9 Dielectric Constant (ε)

The dielectric constant determines how light travels in a material. It is a poor conductor or an insulator. 'The dielectric constant is given by' (Wooten, 1972, Mahrov, *et al.*, 2004) :

$$\varepsilon = \varepsilon_r + \varepsilon_i \qquad 2.19$$

$$\varepsilon = (n + ik)^2 \qquad 2.20$$

$\varepsilon_r and \varepsilon_i$ denotes the real and imaginary parts respectively. Hence,

$$\varepsilon_r = n^2 + k^2 \qquad 2.21$$

and

$$\varepsilon_i = 2ink \qquad 2.22$$

k denotes extinction coefficient and n denotes the refractive index

2.5.10 Optical Conductivity $(\sigma)_o$

According to (Wooten, 1972, Mahrov*et al.*, 2004) 'Optical conductivity (σ_o) is the optical response of a solid material, it is given by as'

$$\sigma_o = \frac{\alpha nc}{4\pi} \qquad 2.23$$

c denotes light velocity.

2.6 Cadmium Sulphide (CdS)

The cadmium sulphide occurs in nature as a substance with two different structures 'greenockite' and 'hawleyite' also as an impurity substituent in zinc ores 'sphalerite' and 'wurtzite'.

According to (Hop, 2008) 'The cadmium sulphide can be prepared by chemical bath deposition technique (CBD)' also by 'electrochemical method as reported' by (Echendu, 2018), and several other methods.

Cadmium sulphide can combine with p-type materials to form the major part of photovoltaic cell. It can also be used as a solid state laser. The cadmium aluminiumsulphite($CdAl_2SO_3$) is a quaternary compound of cadmium, aluminium, sulphur and oxygen. The present work is to grow this thin film and also investigate its properties for appropriate applications.

CHAPTER THREE

MATERIALS AND METHOD

This chapter gives details of the materials used in the growing process, the cleaning processes used and the procedures employed to deposit and characterize the thin films, the equipment used in the characterization.

3.1 Materials for Film Deposition

3.1.1 Chemicals Used for Deposition of Cadmium Aluminium Sulphite Thin Films

Analytical reagent (AR) grade chemicals were used.

For Cadmium aluminium sulphite ($CdAl_2SO_3$) thin films, we used;

i. Cadmium chloride *($CdCl_2$),* as a precursor for cadmium
ii. Aluminiumsulphateoctadecahydrate*($Al_2(SO_4)_3.18H_2O$),* as a precursor for aluminium
iii. Thiourea*($(NH_2)_2CS$,* as a precursor for sulphur
iv. Ethylenediaminetetraacetic acid *(EDTA)* as the complexing agent
v. Ammonia as the PH stabilizer
vi. De-ionised water.

3.1.2 Cleaning of the Substrates

Prior to the deposition, the substrates were degreased by dipping them in concentrated *HCL* for 42 hours, washed with detergent, rinsed with distilled water and dried in air.

3.2 Bath Constituent and Deposition of Film

The reaction bathwas constituted in a 50ml beaker which contains 5ml of 0.75M $CdCl_2$ which was the precursor for cadmium ion. 5ml of 0.9 M of ethylene-diamine-tetraacetic acid (EDTA) the complexing agentwas added to the solution with stirring. After which 5ml of 0.75 M $Al_2(SO_4)_3 .18H_2O$the precursor for aluminium ion was added with stirring. 5ml of 1.5M NH_3 was then emptied into the beaker with continued stirring to provide alkaline medium for the reaction to take place. Finally, 5ml of 0.75M thioureathe precursor for sulphur ion was added and properly stirred. 25ml of distilled water was added to make the solution up to 50ml. The entire solution was stirred very well before the insertion of the glass substrate vertically downward into the beaker with the aid of the synthetic foam for suspension and also prevention of dust and other particles from entering the solution. The reaction parameters such as pH, ionic concentration and period of deposition were optimized. The reaction bath was constituted at room temperature.

The bath was left for about 62 hours, after which the slides were removed, rinsed in distilled water and dried in air. The as-deposited thin films of $CdAl_2SO_3$ were kept in slide box.

3.3 Film Growth Process

According to (Eya&Eze, 2011) 'Chemical bath deposition is a technique for controlling the homogeneous precipitation of water-insoluble compounds and their solid solution'. The growth process involved the reaction of the cations and the anions in the solution bath to form neutral atoms which precipitated as films. For homogenous solution, the bath was constantly stirred.

$CdCl_2$ solution was colourless and transparent until *EDTA* was introduced into the solution, a white precipitate was observed. On the introduction of $Al_2 (SO_4)_3$

.$18H_2O$ the reaction bath bubbled and gave colourless solution . When $NH_3$was added, milky white precipitate was observed which later gave colourless solution. Introduction of thiourea did not affect the colourless nature of the solution. The reaction bath turned white after *90* minutes.

The film growth process basically involved three phases.

i. the incubation phase
ii. the condensation of species or growth phase
iii. the terminal phase.

At the first phase, free positive and negative ions or atoms or molecules were created in the solution with also the creation of nucleation sites. The second phase being the growth phase witnessed the gradual addition of atoms/molecules on the nucleation sites, which gave rise to a whole film formation. The nucleation sites were created by the surface texture of the substrate and enhanced by the systematic cleaning process carried out before deposition. Condensation of the species on the substrate followed after nucleation and continued until all the species were used up in the solution, which eventually gave rise to the final phase, which is the terminal phase. The $CdAl_2SO_3$ solution bath at this point, was clear with white precipitate observed at the bottom of the beaker.

$CdAl_2SO_3$film growth was achieved via ion-by-ion condensation process. This process witnesses the diffusion of Cd^{2+}, Al^{3+}, $S^{2-}$and O^{2-}ions onto the substrate, to form $CdAl_2SO_3$nuclei. The $CdAl_2SO_3$ nucleus grew by the absorption of the ions from the solution. The growth continued till the solution is depleted of ions, leading to the terminal phase.

The chemistry of the reaction is given below.

The reaction between cadmium chloride *($CdCl_2$)*, i.e cadmium precursor and EDTA formed the metallic complex $[Cd(EDTA)]^{2+}$.

$$CdCl_2 + EDTA \leftrightarrow [Cd(EDTA)]^{2+} + 2Cl^- \quad 3.1a$$

The Cd^{2+} was released into the solution by the metallic complex later.

$$[Cd(EDTA)]^{2+} \leftrightarrow Cd^{2+} + EDTA \quad 3.1b$$

Aluminium ion Al^{3+} was released from aluminiumsulphateoctadecahydrate $Al_2(SO_4)_3.18H_2O$ into the solution by the reaction below

$$Al_2(SO_4)_3.18H_2O + (NH_3) \leftrightarrow 2[Al_2(NH_3)]^{3+} + 3(SO_4)^{2-} + 18H_2O \quad 3.2a$$

Then, in ambience

$$2[Al_2(NH_3)]^{3+} + 3O_2 \leftrightarrow 2Al^{3+} + 6O^{2-} + NH_3 \quad 3.2b$$

The precursor for sulphur ion is $(NH_2)_2CS$ of which the hydrolysis gives S^{2-}, according to Eqs 3.3a and 3.3b.

$$(NH_2)_2CS + OH^- \leftrightarrow (NH_2)_2CO + HS^- \quad 3.3a$$

$$HS^- + OH^- \leftrightarrow S^{2-} + H_2O \quad 3.3b$$

Then the four ions react giving:

$$Cd^{2+} + 2Al^{3+} + 3O^{2-} + S^{2-} \leftrightarrow CdAl_2SO_3(\downarrow) \quad 3.4$$

Thus the whole process of deposition gives

$$[Cd(EDTA)]^{2+} + 2[Al_2(NH_3)]^{3+} + (NH_2)_2CS + 2OH^- + 3O^{2-} \leftrightarrow CdAl_2SO_3(\downarrow) + EDTA + (NH_2)_2CO + NH_3 + H_2O \quad 3.5$$

The reaction of $equation$ 3.4 is only possible when the ionic product, IP of Cd^{2+}, Al^{3+}, $O^{2-}$and S^{2-} exceeds solubility product, K_{sp} *of* $CdAl_2SO_3$, i.e., when

$$[Cd^{2+}][\,Al^{3+}][O^{2-}][\,S^{2-}] > K_{sp}(CdAl_2SO_3) \qquad 3.6$$

The $CdAl_2SO_3$ nucleus grew by absorption of Cd^{2+}, Al^{3+}, S^{2-} and O^{2-} and ions from the solution and the growth continued until the solution is depleted of ions.

The complexing agent which gave good deposition for the reaction was ethylene-diaminetetraacetic acid (*EDTA*), when tri-ethanolamine (*TEA*) was tried no deposition was formed on the substrate, also when *EDTA* + *TEA* was used no deposition was seen on the substrate. *EDTA* formed a complex with cadmium, i.e., $[Cd\ (EDTA)]^{2+}$ and also, ammonia formed a complex with aluminium, i.e., $[Al\ (NH_3)_3]^{3+}$. The formation of metallic complex also slowed down the reaction to enable proper and smooth deposition of films on the substrate.

3.4 Structural Characterization

The structural characterization was done with the use of glancing incident X-ray diffraction (GIXRD) and Raman spectroscopy.

The XRD measurement was done with theRigaku Smart Lab X-Ray diffractometer with CuK alpha (wavelength = 1.5406 A) and the Raman measurement was carried out by A WITec Alpha 300R confocal Raman Microscopy machine with laser wavelength of 514nm in Physics Lab., Department of Physics, City university of Hong Kong.

3.5 Optical and Solid State Characterization

The optical and solid state properties of the thin films for complete characterization of this work include: absorbance (A), transmittance (T), reflectance(R), absorption coefficient(α), band gap energy (E_g), refractive index (n), extinction coefficient (k), dielectric constant (ε) imaginary and real parts, optical conductivity(σ_o). The transmittance and reflectance were gotten from the use of MPROBEUV-Vis-NIR spectrophotometer optical measurement system, carried out in Physics Lab., Department of Physics, City university of Hong Kong. The characterization was done within the UV-Vis-NIR region of the electromagnetic spectrum. The absorbance was calculated using equation 1.6. The absorbance, transmittance and reflectance spectrum were used for the determination of other parameters. The absorption coefficient was calculated using$equation$ 1.8. Optical density and band gap were calculated using $equations$ 1.13 and 1.18 respectively. Refractive index was computed using $equation$ 1.12, extinction coefficient was by$equation$ 1.23. The real and the imaginary parts of dielectric constant were gotten by $equation$ 1.26 and 1.27 respectively. The optical conductivity was computed using $equation$ 1.28.

3.6Compositional Properties and Thickness

The compositional analysis was done in Physics Lab., Department of Physics, City University of Hong Kong. Using EDAX ^{TSL}Advanced microanalysis solutions AMETEK and the 3D optical profilometry method was used for films thickness measurement inPhysics Lab., Department of Physics, and City University of Hong Kong by Filmetrics Profilm3D equipment.

3.7 Morphological Properties

The morphological analysis was carried out using Scanning Electron Microscope (SEM). The analysis was done in Physics Lab., Department of Physics, City university of Hong Kong using FEI SEM XL30.

3.8 Annealing of $CdAl_2SO_3$ Samples

The annealing was carried out in the Material/Metallurgical Engineering Laboratory, Federal University of Technology, Owerri. Using Electrothermal Oven, SearchTech Instrument, Model DHG.The samples were annealed as follows;

Table 3.1 Annealed samples for $CdAl_2SO_3$thin films material.

Samples	Annealing temperatures
C1 and G1	100°C
C2 and G2	150°C
G3 and N3	200°C
C3 and N5	230°C
G10 and N12	250°C

Some of the as-deposited and annealed samples are given in the plates below.

Plate 1 Photograph of *$CdAl_2SO_3$* thin films samples

CHAPTER FOUR

RESULTS AND DISCUSSION

Cadmium aluminiumsulphite ($CdAl_2SO_3$) is a quaternary nanocrystallite thin films. The thin films are white in colour and strongly adherent to the substrate. The original intension was to grow a ternary thin film of cadmium aluminiumsulphide (CdAlS) but after the characterization, it was observed that the samples are oxygen rich. From the XRD results, the samples were identified as $CdAl_2SO_3$.

4.1 Film thickness and Compositional Analysis

3D optical profilometery method was used to determine the films thickness of the materials. It is observed that the films thickness generally decreases with increasing annealing temperature.

The as-deposited sample has films thickness of 879nm and the annealed samples have films thicknesses of 288nm, 332nm and 207nm for annealing temperatures of 150°C, 200°C and 250°C respectively.

The graph of thickness against annealing temperature is given in figure 4.1. From the graph, it is observed that at about 27°C i.e. room temperature, the thin films material has the highest value of thickness given as 879nm. Above the room temperature, at annealing temperature of 150°C, there is sharp decrease in thickness. As the annealing temperature increases the thickness decreases. At annealing temperature of 150 °C there is sharp decrease in thickness with the value of 288 nm. At annealing temperature of 200 °C, the thickness increases to 332 nm. And then, at the annealing temperature of 250 °C the thickness falls to 207 nm. The material dependence on annealing temperature is not uniform. The optimal annealing temperature for thickness is 200 °C. For the samples, the as-deposited material gives a better option for photonic applications.

The elemental composition analysis was carried out using energy dispersive X-ray (EDX) spectroscopy. Figure 4.14 shows the energy dispersive X-ray spectra of the $CdAl_2SO_3$ in both as-deposited and annealed forms. The spectra show the presence of Cd, Al, S and O. Other peaks showing C, N and part of O come from the underlying glass substrate on which these films are grown.

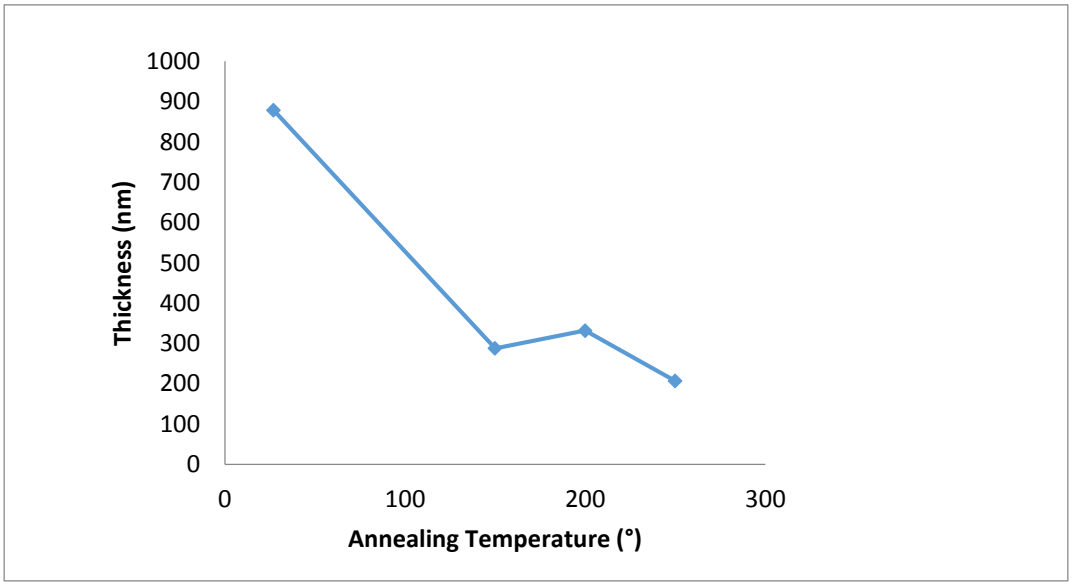

Figure 4.1 The graph of thickness against annealing temperature.

Close observation of the spectra shows a slight decrease in sizes of the peaks, after post-deposition annealing of the material. This also reaffirms the fact that post deposition annealing reduces the thickness of the films as stated above.

Table 4.1 shows the percentage atomic concentrations of Cd, Al, S and O in the materials gotten from the analysis of EDX. Fig. 4.2 and Table 4.1 show that as-deposited and annealed materials are Al and O-rich. The CdS/O ratio for as-deposited sample is slightly higher than that of the annealed samples. The same trend is repeated for Al/O ratio for both as-deposited and annealed samples.

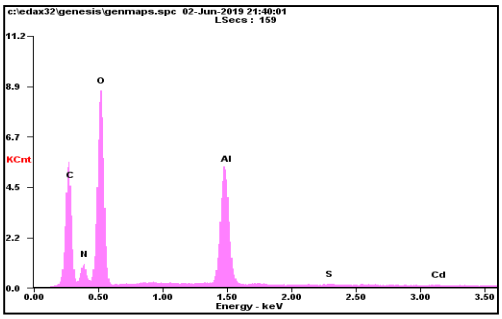

As-deposited

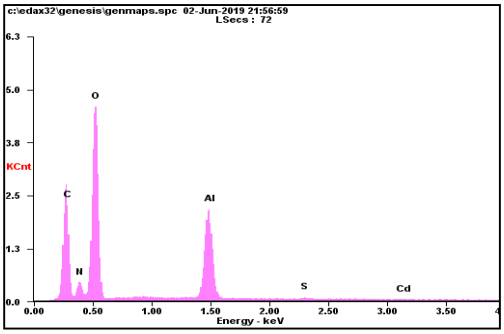

150°C Annealed

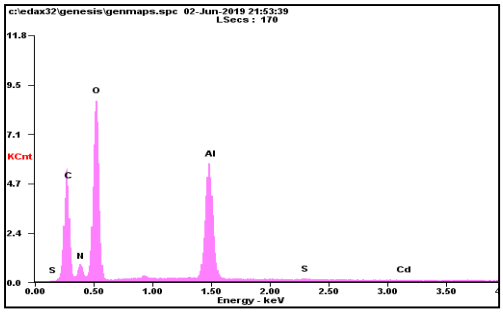

230 ° C Annealed

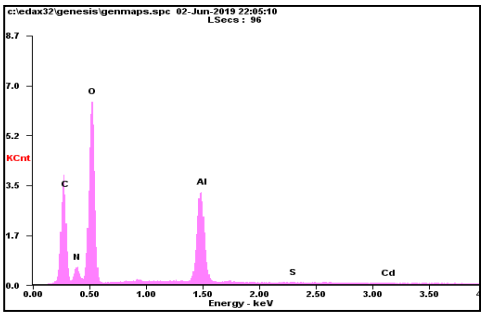

250 ° C Annealed

Figure 4.2 EDX spectra of as-deposited and annealed *$CdAl_2SO_3$* thin films grown by CBD method

Table 4.1 Percentage atomic compositions of as-deposited and annealed $CdAl_2SO_3$ thin films

As-deposited							Annealed					
Atomic %							Atomic %					
Cd	Al	S	O	CdS/O	Al/O		Cd	Al	S	O	CdS/O	Al/O
0.1	16.08	0.15	83.7	0.0002	0.19	150°C	0.08	13	0.18	86.74	0.00017	0.15
						230°C	0.04	16.97	0.12	82.87	0.000058	0.20
						250°C	0.06	14.27	0.1	85.57	0.000071	0.17

4.2 Morphological Analysis

The scanning electron microscopy is a convenient method for studying the surface morphology of a material. Figure 4.3 shows SEM micrographs of the as-deposited and annealed $CdAl_2SO_3$ thin films samples. These images show that the post-deposition annealing has little effect on the morphology of the $CdAl_2SO_3$ samples. It is observed that the grains are homogenous and densely packed. It is also noticed that the grains are small with unequal sizes and shapes with sharp edges showing crystallinity. Isolated clusters were also observed from the SEM images of the materials especially for annealed samples.

Due to the dense nature of the grains, it was difficult to measure grain sizes. However, close observation and careful estimation gave the grain sizes of the range (20-70) µm for the as-deposited sample and (15-50) µm for annealed samples. These values show that the material sizes decrease with increasing annealing temperature.

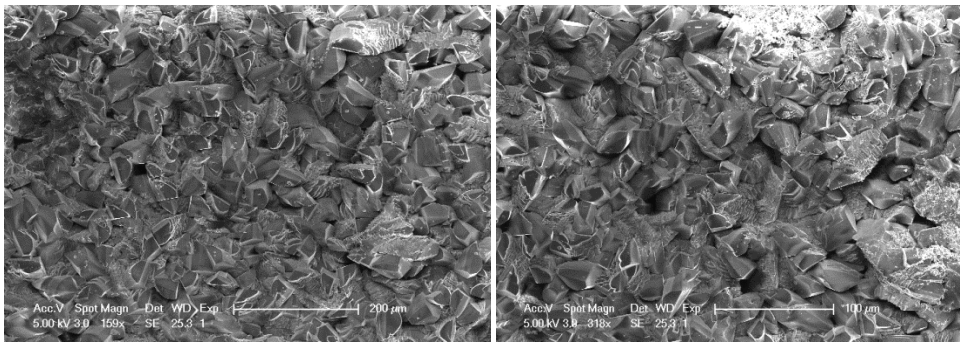

A1 As-deposited ×159 A2 As-deposited ×318

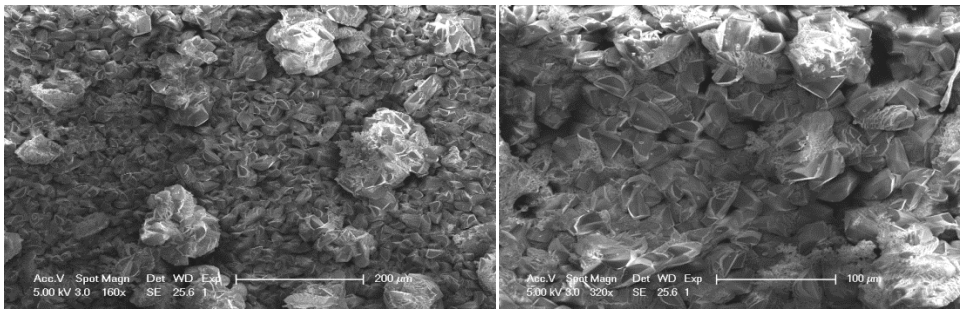

B1-150°C Annealed ×160 B2-150°C Annealed ×320

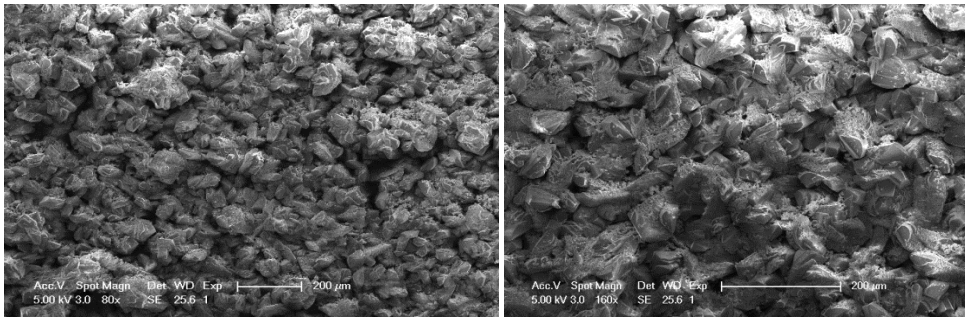

C1-200°C Annealed ×80 C2-200°C Annealed ×160

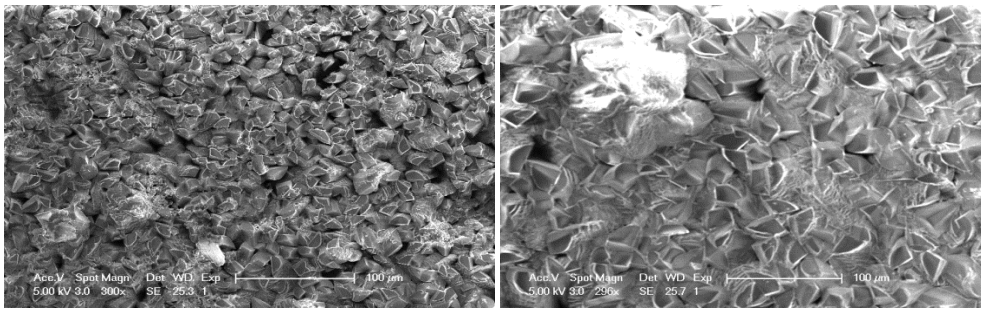

D1-250°C Annealed ×300 D2-250°C Annealed ×296

Figure 4.3 SEM images of as-deposited and annealed $CdAl_2SO_3$ thin films grown by CBD method

4.3 Structural Analysis of $CdAl_2SO_3$

Close observation of the glancing incident X-ray diffractionGIXRD graph and Raman graph from figure 4.4 and 4.5 respectively show sharp peaks indicating that the material is a crystalline material.

The GIXRD pattern clearly show that the quaternary material cadmium aluminiumsulphite ($CdAl_2SO_3$) forms as a multi-phased compound with a combination of $CdSO_3$ (monoclinic) and Al_2O_3(monoclinic) as indicated by the diffraction peaks corresponding to these materials in both as-deposited and annealed forms in figure 4.4. The diffraction patterns match those of the Joint Committee on Powder Diffraction and Standard (JCPDS) ref. file number PDF 781474 and PDF 861410, respectively. Multiphase thin film materials had been reported by many researchers: (Echendu*et al*, 2018, Cheng *et al*, 2017, Bakke *et al*, 2012, Polat*et al*, 2011, Henriquez *et al*, 2007).

The as-deposited material has the intensity with the highest peak at about 10000 (arb. unit). At annealing temperature of 150°C, no noticeable change of the intensities of the peaks were observed as the highest peak is still at the region of 10000 (arb. unit) intensity. At 200°C the highest peak rose to about 15000(arb. unit) and at 250°C the highest peak rose to about 20000 (arb. unit) intensity. These simply show that increase in annealingtemperature increases the preferential orientation of the crystallites of the material. The increment of the annealing temperature also gave improved crystallization indicated by narrower peaks shown by the reduction in width for full width at half maximum (FWHM).

The highest peak has the value of 2θ equal to 12.6degrees with the orientation of (011) which is the preferred orientation of the crystallite (atoms) for both as-deposited and annealed material.

The crystallite size (D) using the major peaks was calculated using Scherrer's equation 4.1.

$$D = \frac{0.94\lambda}{\beta cos\theta} \qquad 4.1$$

Where λ is the wavelength of the X-ray and is equal to 1.5406 $\dot{A}$, β is the full width at half maximum of the diffraction peak (in radians) and θ is the Bragg's angle in degrees.

The interplanar spacing, d, is calculated using the Bragg equation 4.2.

$$d_{hkl} = \frac{n\lambda}{2sin\theta} \qquad 4.2$$

Where λ is the X-ray wavelength, θ is the diffraction angle and n is an integer.

Table 4.1 shows the summary of the structural parameters obtainable from the GIXRD analysis for $CdAl_2SO_3$ using Eqs 4.1 and 4.2.

Figure 4.5 shows the Raman spectrum of as-deposited and annealed$CdAl_2SO_3$ material. Raman bands results directly from molecular vibrations. These vibrations reveal the chemical and structural composition of samples. The frequency of vibration depends on the masses of the atoms and the strength of the bonds between them. 'Heavy atoms and weak bonds have low Raman shift and light atoms and strong bonds have high Raman shift. The Raman spectrum consists of a range of features, each associated with a vibrational mode. The spectrum is unique to a material and enables you to identify it'. (www.renishaw.com). From the Fig. 4.5, we have high frequency vibrations (Raman peaks) in the region of 2500$cm^{-1}$and 3000cm^{-1}andlow frequency vibrations (Raman peaks) in the region of 1$cm^{-1}$and 700$cm^{-1}$for the as-deposited material. For annealed materials at 150°C and 200°C these frequency vibrations reduced significantly, but at 250°C however these vibrations frequency begin to rise especially around the wavenumber 3000cm^{-1}.This high frequency vibration shows that we have light material with strong bonds.

The bond pattern is however, not achieved since there is no reference database for identification of material.

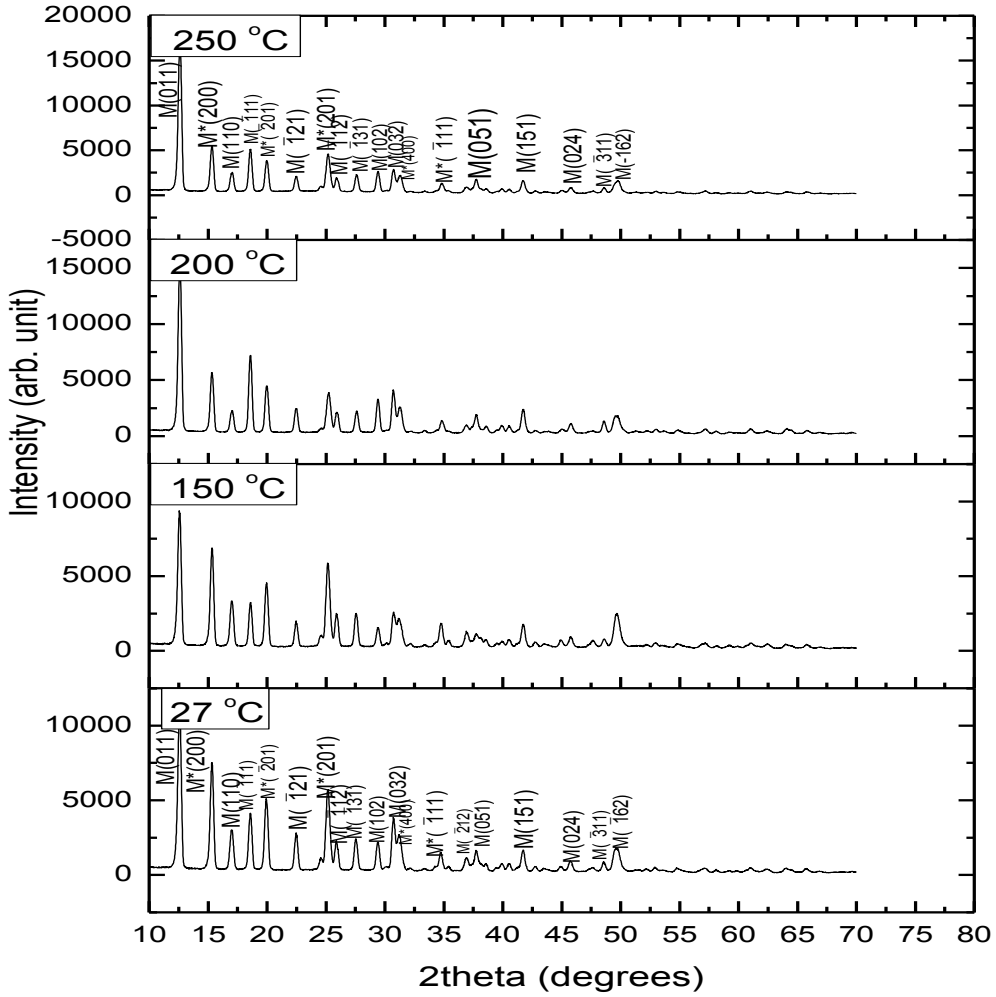

Figure 4.4 GIXRD patterns of as-deposited and annealed$CdAl_2SO_3$ thin films, showing monoclinic $CdSO_3$ (M) and Al_2O_3 (M*).

The structural parameters obtained from the GIXRD patterns for the*$CdAl_2SO_3$* thin films in both as deposited and annealed form is given in table 4.2. The table shows mixture of $CdSO_3$ (monoclinic) and Al_2O_3 (monoclinic) planes of different

orientations; with prefer orientation of (011).The table also gives the full width at half maximum for as deposited and annealed material having comparable values as well as inter-planar spacing, but the inter-planar spacing decreases as the 2theta values increases for both as deposited and annealed thin films material. However, the crystallite sizes slightly increase afterpost-deposition annealing of the thin film materials.This could be due to decrease in full width at half maximum after annealing.The crystallite nanoscale size suggests that the material could be used as quantum dots.

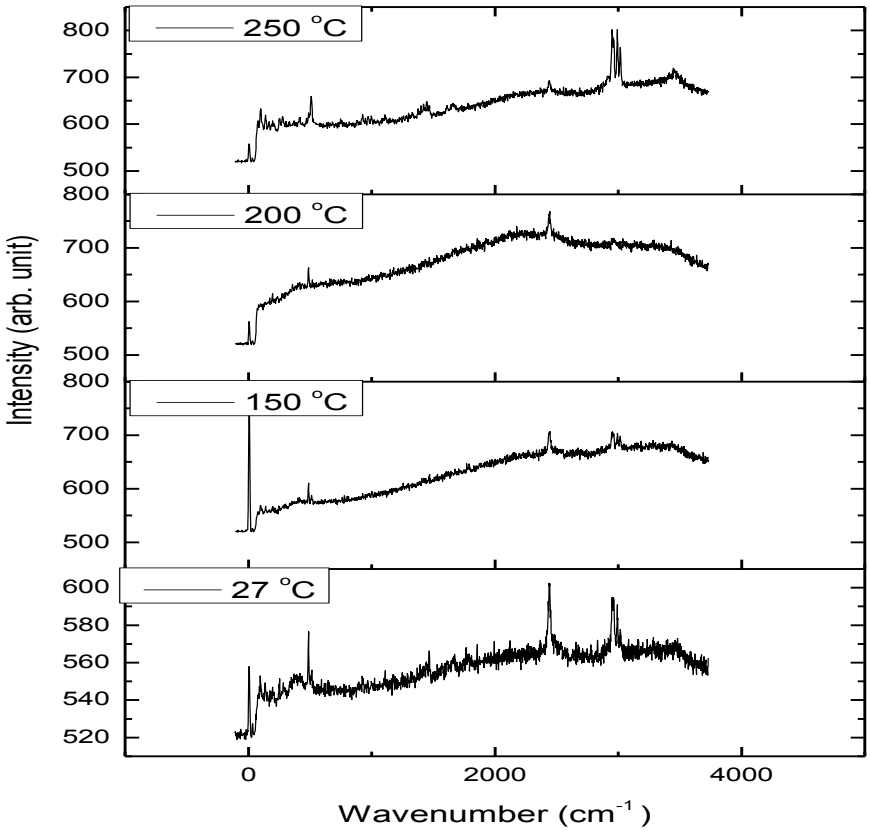

Figure. 4.5Raman peaks of as-deposited and annealed $CdAl_2SO_3$ thin films

Table 4.2 Crystal structure parameters of as-deposited and annealed$CdAl_2SO_3$ thin films.

As-deposited					Annealed					
2θ (°)	(hkl)	β (°)	d-spacing (Å)	D (nm)		2θ (°)	(hkl)	β (°)	d-spacing (Å)	D (nm)
12.6	M(011)	0.3632	7.02	22.99	150°C	12.6	M(011)	0.3544	7.02	23.56
15.3	M*(200)	0.3451	5.79	24.26		15.3	M*(200)	0.3633	5.79	24.82
17.0	M(110)	0.3676	5.21	22.83		18.6	M($\bar{1}$11)	0.3292	4.77	25.54
18.6	M($\bar{1}$11)	0.3597	4.77	23.38		19.9	M*($\bar{2}$01)	0.3317	4.46	25.40
19.9	M*($\bar{2}$01)	0.3482	4.46	24.20		25.1	M*(201)	0.3975	3.55	21.39
22.5	M($\bar{1}$21)	0.3461	3.59	24.45	200°C	12.6	M(011)	0.3520	7.02	23.72
25.2	M*(201)	0.4089	3.53	20.8		15.3	M*(200)	0.3633	5.79	23.05
27.5	M($\bar{1}$31)	0.3645	3.24	23.45		18.6	M($\bar{1}$11)	0.3473	4.77	24.21
30.7	M(032)	0.4093	2.91	21.03		20.0	M*($\bar{2}$01)	0.3537	4.44	23.83
						25.2	M*(201)	0.4581	3.53	18.56
M = $CdSO_3$ Monoclinic					250°C	12.6	M(011)	0.3412	7.02	24.47
M* = Al_2O_3 Monoclinic						15.3	M*(200)	0.3367	5.79	24.87
						18.6	M($\bar{1}$11)	0.3329	4.77	25.26
						19.9	M*($\bar{2}$01)	0.3350	4.46	25.15
						25.2	M*(201)	0.4023	3.53	21.14

Parameters for the JCPDS reference file 781874, i.e. $CdSO_3$ 2θ = (12.7, 17.7, 19.1, 22.8, 27.8, 30.2) ° and JCPDS reference file 861410, i.e. Al_2O_3 2θ = (15.5, 19.6, 25.1) ° respectively.

4.4 Optical Properties of $CdAl_2SO_3$ Thin film

The optical characterization result for the $CdAl_2SO_3$ thin films are presented below.

4.4.1 Transmittance (T)

Figure 4.6 shows graph of the transmittance against wavelength for the as-deposited and post-deposition annealed nanocrystallite $CdAl_2SO_3$ thin films.

The as-deposited material has a transmittance of about 3.5 % in the NIR-region which increases to about 3.9 % in the Vis-region and falls in the UV-region. The

200 °C annealed sample has about 4.6 % transmittance in the NIR-region which rises to about 5 % in the Vis-region and falls in the UV-region. The 250 °C annealed sample has about 5 % in the NIR-region which increases to about 6 % in the Vis-region and falls in the UV-region of the solar spectrum. These show that the transmittance of the nanocrystallite material is slightly affected by annealing temperature. That is, increase in annealing temperature increases transmittance.

Generally, the transmittance of the thin films is uniform in the NIR-region which rises slightly towards the Vis-region and falls across the UV-region of the solar spectrum. The reason for poor transmittance being that the material is an opaque material. This poor transmittance shows that the material will not be a good window material for thin films solar cells but suggests that it will be very good for solar absorber material in thin films solar cells.

4.4.2 Absorbance (*A*)

The graph of optical absorbance versus wavelength for as-deposited and post-deposition annealed $CdAl_2SO_3$ thin films material is shown in figure 4.7, for the wavelength range of 300nm to 900nm. From the figure, the highest absorption occurs at the UV-region of the electromagnetic spectrum, with as-deposited sample having absorption of about 99.5% at wavelength of 300nm, followed by 250°C annealed sample with absorption of about99.3% , followed by 200°C annealed film with the absorption of about99%, and fianlly 150°C annealed film with absorption of about98.8%, respectively all at 300nm wavelength.

We observed that absorption in the UV-spectrum is exact reversal of the absorption in the visible-near infrared spectrum for annealed materials only. The 250°C annealed sample that is the highest annealed in the UV-spectrum is the lowest in

the Vis-NIR spectrum falling to about 94%, followed by 200°C sample that falls to about 94.5%, and finally 150°C sample that falls to about 95% in that order.

The as-deposited material maintained the lead absorbance of99.5%in the UV-region and Vis-NIR region. This reaffirms that annealing condition used did not increase the absorbance of the thin material. The material gives optimum absorbance in as-deposited form.

Due to the very high absorbance of the $CdAl_2SO_3$, it is suited for absorber material for thin films solar cells. The material can also be used in UV-shielding due to its high absorption in the UV-spectrum.

4.4.3 Reflectance (*R*)

Figure4.8 shows the reflectance against wavelength for as-deposited and post-deposition annealed $CdAl_2SO_3$ thin film material. The material generally has very low reflectance for as-deposited and annealed samples across the UV-Vis-NIR regions of the solar spectrum. The reflectance is lower in the UV-regioncompared to Vis-NIR region. The 250°C annealed sample has the lowest reflectance in both UV and Vis-NIR region. It has about 0.3% reflectance in the UV which rose to about 1% in the visible and falls to about 0.6% in the NIR-region. The 200°C annealed sample has about 0.7% in the UV, which rose to about 1.3% in the visible, and falls to about 0.8% in the NIR-spectrum. The 150°C annealed sample has 0.9% in the UV which rose to 1.5% in the visible and falls back to 1.0% in the NIR-region.

The as-deposited sample also have the same behaviour as the annealed samples taking low value of reflectance in the UV-region, then rising in the visible region and falling in the NIR-region with the values of 0.4% in the UV, 1.2% in the visible and 0.8% in the NIR-region.

The poor reflectance property makes the material very good for anti-reflection applications.

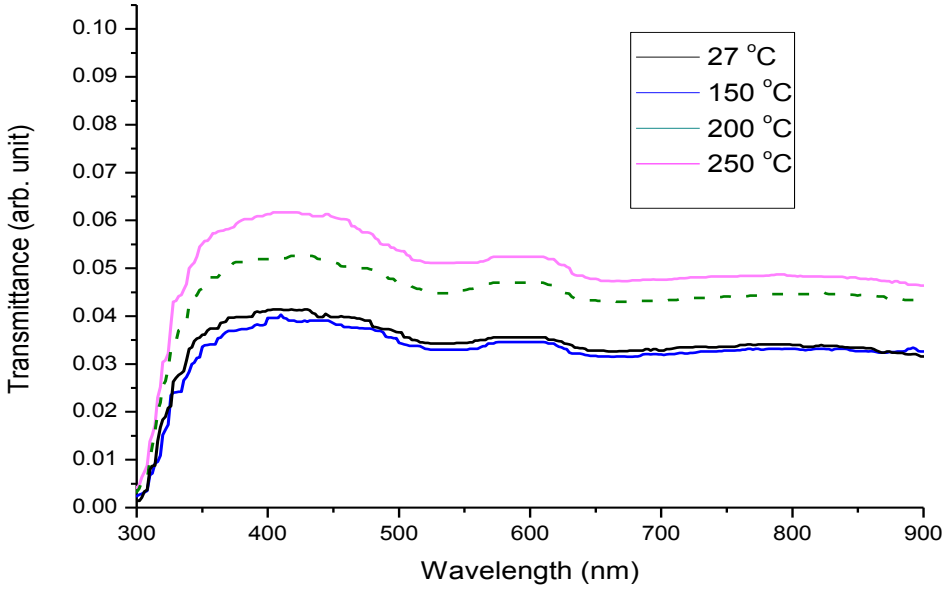

Figure 4.6 Graph of optical transmittance against wavelength for as-deposited and post-deposition annealed $CdAl_2SO_3$ thin films

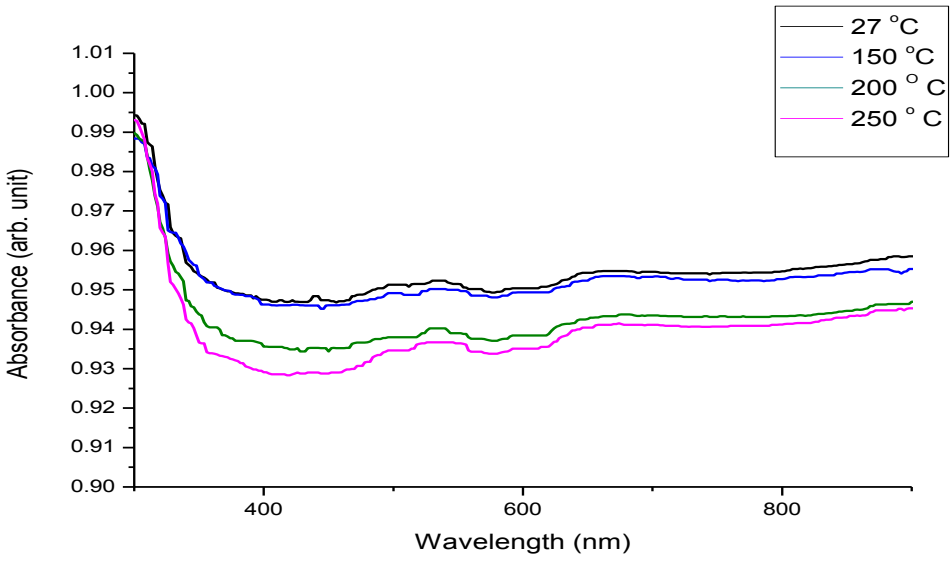

Figure 4.7Graph of optical absorbance against wavelength for as-deposited and post-deposition annealed $CdAl_2SO_3$ thin films

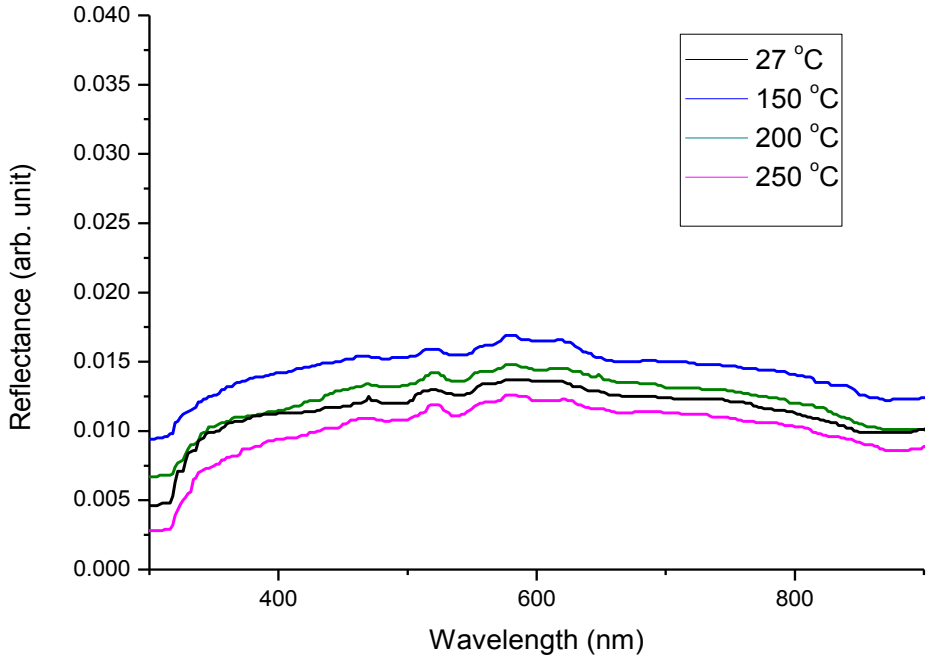

Figure 4.8Graph of optical reflectance versus wavelength for as-deposited and post-deposition annealed *$CdAl_2SO_3$* thin films

4.4.4 Absorption Coefficient (α)

The graph of absorption coefficient against photon energy for both as-deposited and annealed $CdAl_2SO_3$ thin films is shown in figure 4.9. It is observed that the absorption coefficient for the annealed materials is higher than that of the as-deposited material. This could be due to increase in density of the films when annealed. The as-deposited material has absorption coefficient of about $6.0 \times 10^6 m^{-1}$ close to the absorption edge (3.68 eV) of photon energy. The annealed materials have the absorption coefficient in the range of $12.5 \times 10^6 m^{-1}$ to$21.0 \times 10^6 m^{-1}$close to the absorption edge of the solar spectrum. The absorption coefficient is fairly uniform for both annealed and as-deposited materials in NIR-Vis (1.4 eV-1.7eV, 1.7eV-3.1eV) regions of the electromagnetic region, but rises in the far UV-region (3.5 eV – 4.1 eV). The as-deposited material has its highest α of about $6.0 \times 10^6 m^{-1}$

at photon energy of 4.0eV. The annealed materials have their highest absorption coefficient α in the range of 12.5 × $10^6 m^{-1}$to21.0 × $10^6 m^{-1}$ at the same photon energy of 4.0 eV. The trend shows that absorption coefficient increases with annealing temperature. The best annealing temperature for the material with the highest absorption coefficient is 250 °C. Generally, the material has high absorption coefficient which increases as photon energy increases. This again suggests that the material will be a good solar absorber for thin films solar cells.

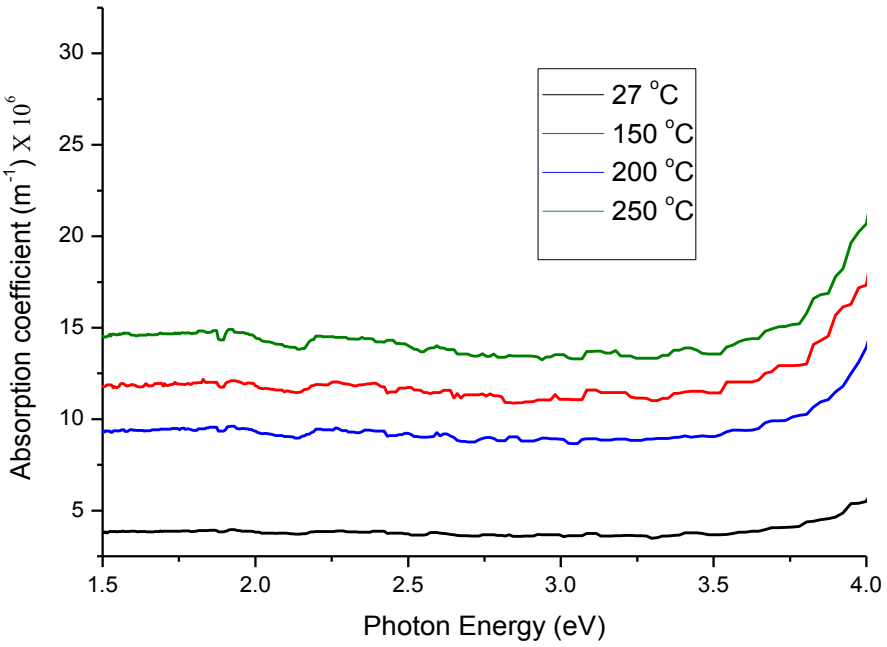

Figure 4.9Graph of absorption coefficient (α) versus Photon energy for as-deposited and annealed *$CdAl_2SO_3$* thin films

4.4.5 Extinction Coefficient (*k*)

Figure 4.10 shows the graph of extinction coefficient against photon energy for both as-deposited and post-deposition annealed $CdAl_2SO_3$ thin film materials. The materials have high extinction coefficient across the Vis-NIR regions. The lowest extinction coefficient starts in the UV-region which gradually increases towards

the visible region (1.7eV – 3.1eV) and has its highest value in the NIR-region (1.4eV – 1.7eV)for both as-deposited and post-deposition annealed samples. This means that the photons are absorbed more in the UV-region.

The as-deposited material has a lower extinction coefficient when compared to the post-deposition annealed samples. The as-deposited sample has its highest extinction coefficient of 2.5 at photon energy of 1.5eV, while the highest extinction coefficient for the post-deposition annealed samples is 0.95 at photon energy of 1.5eV for the 250°C sample.

The value of k for both as-deposited and annealed samples decreases as photon energy increases up to photon energy of 3.8eV, after which it begins to increase. The extinction coefficient generally decreases with photon energy.

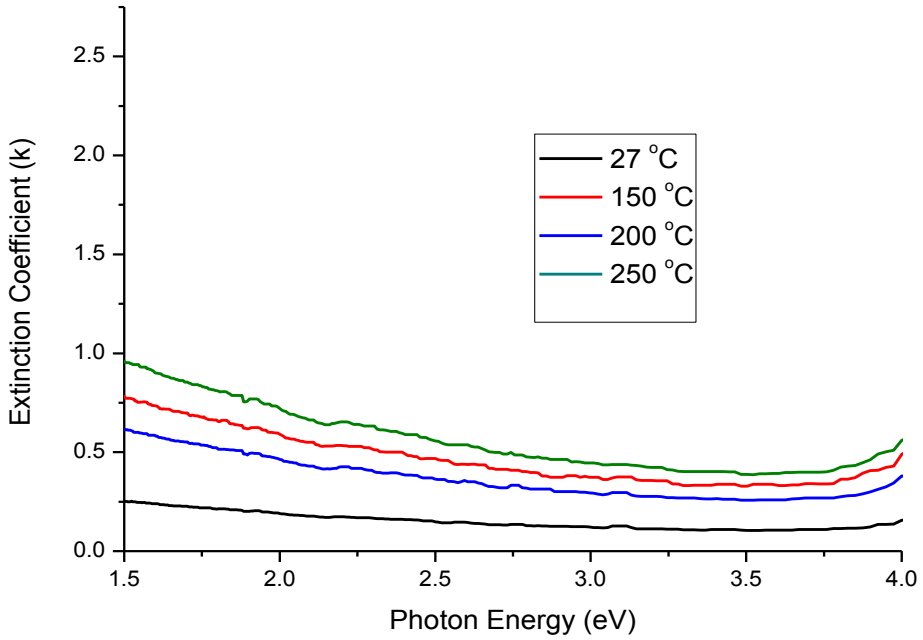

Figure 4.10Graph of extinction coefficient (k) against Photon energy for as-deposited and annealed *$CdAl_2SO_3$* thin films

4.4.6 Refractive Index (n)

Figure 4.11 shows the graph of refractive index against photon energy for both as-deposited and post-deposition annealed $CdAl_2SO_3$ thin films. In general, refractive index increases as photon energy increases until it attains a peak at 2.25eV, and begins to fall with further increase in photon energy.

The refractive index of as-deposited is 1.21 at photon energy of 1.0eV in the NIR-region and rises to 1.40 in the visible at photon energy of 2.25eV which stood as a major spike, with minor spike on the left at photon energy of 2.0eV and two minor spikes on the right at photon energies of 2.5eV and 2.8eV respectively. The post-deposition annealed samples follow a similar trend. The highest refractive index for annealed samples is 1.43, at photon energy of 2.25eV.

Generally, the refractive index for $CdAl_2SO_3$ thin films material is relatively low, and according to the relation $n=c/v^2$ (Echendu*et al*, 2014), where v is the propagation speed of light in the medium, and c is speed of light in vacuum. The relation shows that decrease in refractive index will increase the speed of light propagation in the $CdAl_2SO_3$ thin films material. Also, the low refractive index means that there will be very low reflection loss when $CdAl_2SO_3$ material is used for thin films solar cells material.

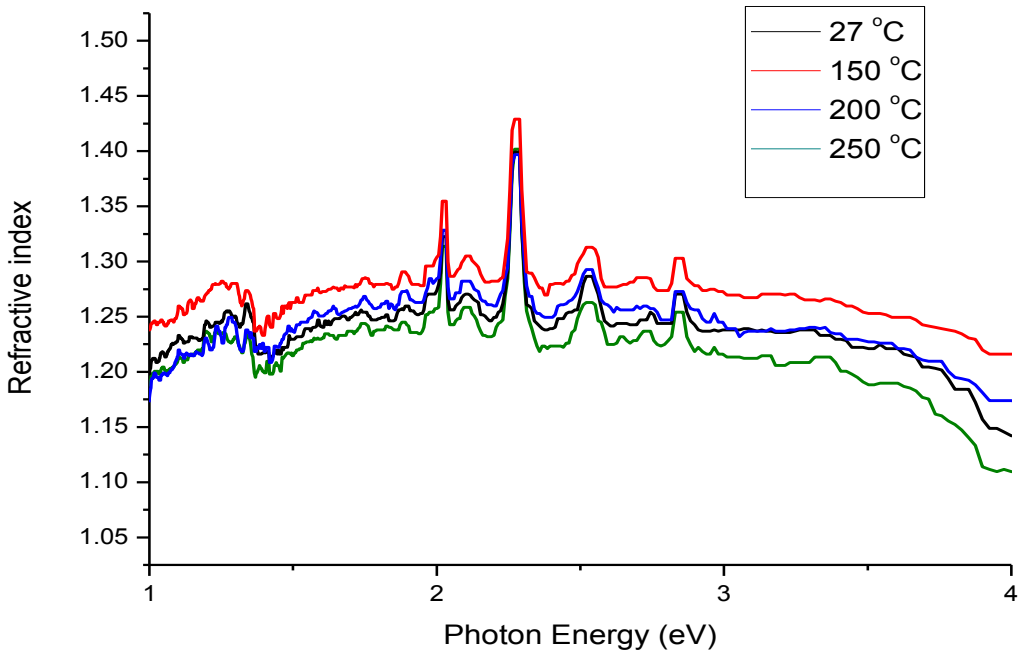

Figure 4.11Graph of refractive index (n) against photon energy for as-deposited and annealed $CdAl_2SO_3$ thin films

4.4.7 Optical Density (ρ)

The optical density versus photon energy for as-deposited and post-deposition annealed $CdAl_2SO_3$ thin films is shown in figure 4.12. The spectral optical density for the material generally decreases with annealing temperature, but increases with photon energy towards the UV-region (3.1eV - 4.1eV) of the electromagnetic spectrum.

The optical density is very low for both as-deposited and post-deposition annealed samples with the highest value for as-deposited being -0.3 at the photon energy of 4.1eV, while 200 °C annealed sample has the highest value of optical density for annealed samples with -0.28 at the photon energy of 4.1eV. Low optical density will fasten light propagation in the thin films material.

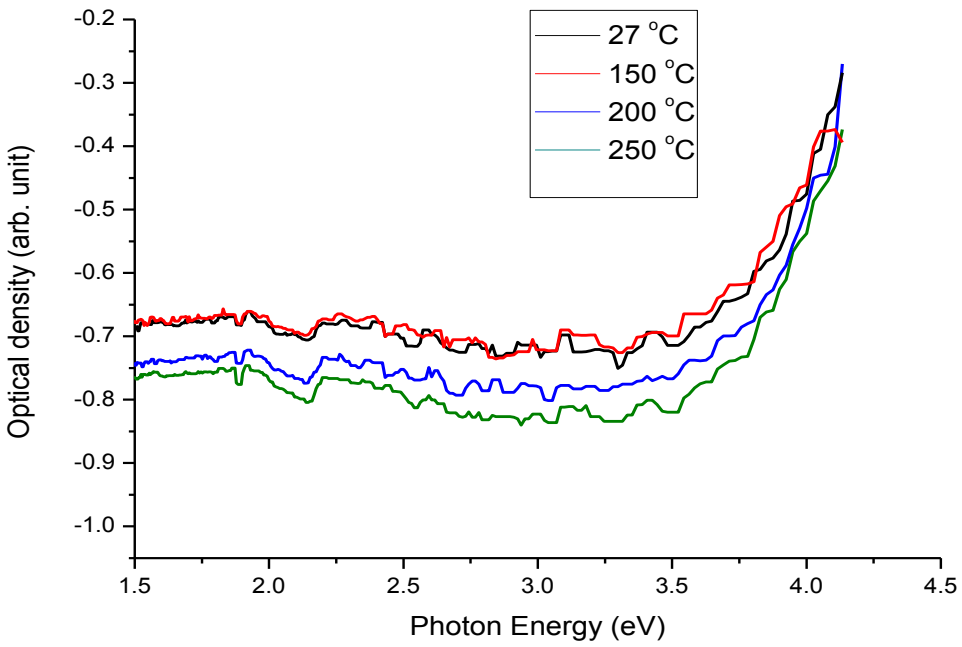

Figure 4.12Graph of optical density versus photon energy for as-deposited and annealed $CdAl_2SO_3$ thin films

4.4.8 Optical Conductivity (σ_o)

The optical conductivity versus photon energy for as-deposited and post-deposition annealed $CdAl_2SO_3$ thin films shown in figure 4.13.The $CdAl_2SO_3$material has a very high optical conductivity which increases with annealing temperature and also with photon energy towards the UV-region (3.1eV – 4.1eV) of the electromagnetic spectrum. The as-deposited sample has its highest value of $1.5 \times 10^{14}(s^{-1})$ optical conductivity at the photon energy of 4.0eV, while the 250°C annealed sample has the highest value of the annealed samples with optical conductivity of $5.4 \times 10^{14}(s^{-1})$ at photon energy of 4.0eV. There are noticeable spikes for as-deposited and annealed materials at photon energy of 2.25eV.

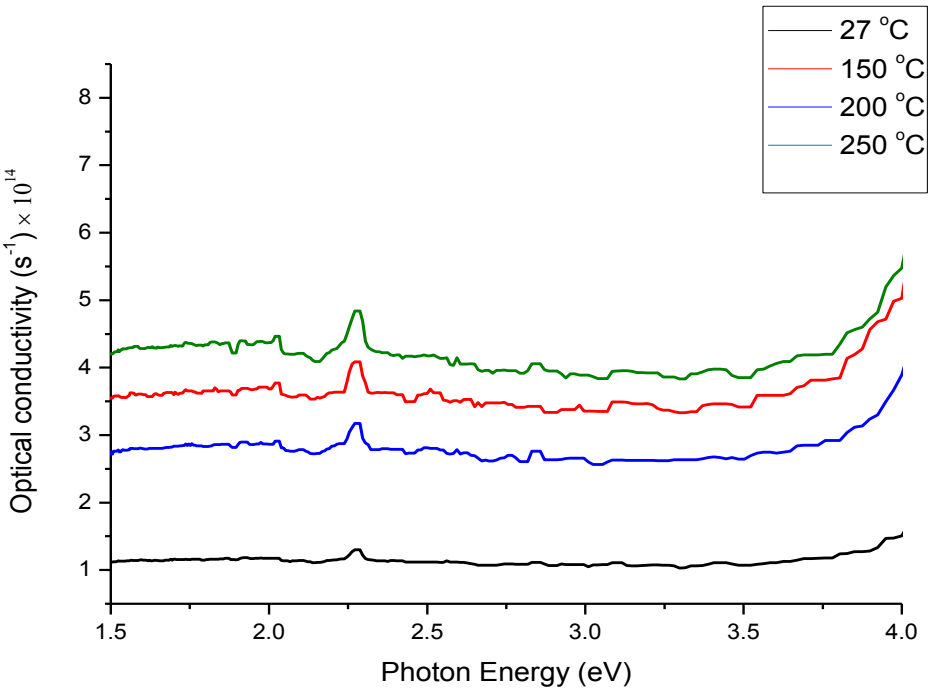

Figure 4.13Graph of optical conductivity versus photon energy for as-deposited and annealed $CdAl_2SO_3$ thin films

4.5 Solid State Properties

The solid state properties investigated in this work are given below.

4.5.1 Dielectric Constants (ε_r and ε_i)

The spectral response of the real dielectric constant ε_r with photon energy for both as-deposited and post-deposition annealed $CdAl_2SO_3$ thin film materials is shown in figure 4.14. The graph shows the same trend as that of the refractive index given in figure 4.11.The real part of the dielectric constant ε_r decreases with increasing annealing temperature.

In general, ε_r for as-deposited and post-deposition annealed material is lower in the NIR-region (lower energy region) and gradually rises in the visible region with a huge spike at 2.25eV, which later slightly decreases in the UV-region of the electromagnetic spectrum in relation to photon energy.

The highest value of the real dielectric constant for as-deposited material is 1.9 at photon energy of 2.25eV which stood as a major spike, with minor spike on the left at photon energy of 2.0eV and two minor spikes on the right at photon energy of 2.5eV and 2.8eV respectively. The highest range of values for post-deposition annealed samples is 1.5 to 1.75 at photon energy of 2.25eV.Low dielectric constants favour light propagation in the material medium.

‘ Low dielectric constant in the lower energy region means that devices made with these layers will exhibit relatively low capacitance and thus will display short response time in this photon energy region, recalling that the response time, t, is related to the capacitance, C, and resistance, R, by t =2.2RC’ (Echendu et al, 2014, Quimby, 2006). This material could thus be used in photodetectors.

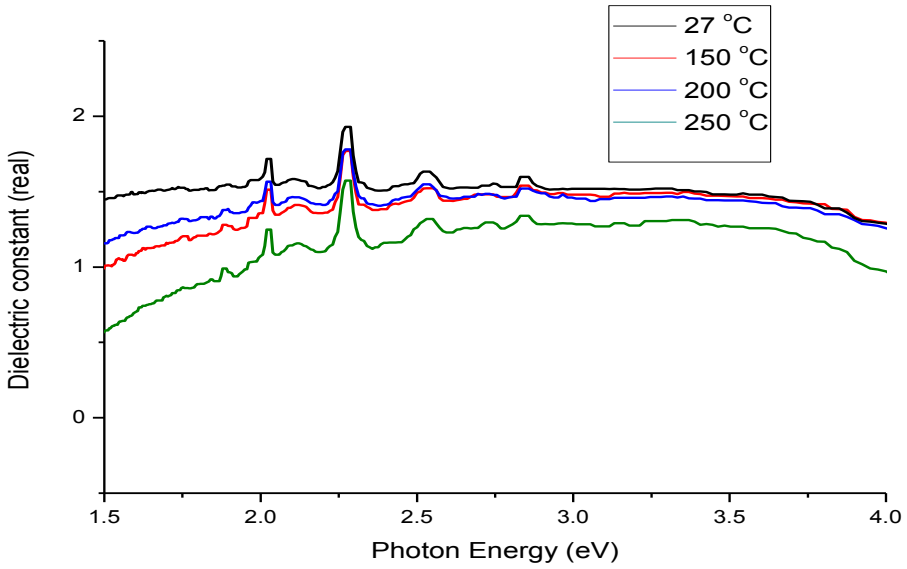

Figure 4.14 The spectral response of the real dielectric constant ε_r versus photon energy for as-deposited and post-deposition annealed $CdAl_2SO_3$ thin films

The optical response of the imaginary dielectric constant against photon energy for as-deposited and post-deposition annealed $CdAl_2SO_3$ thin film materials is given in

figure 4.15. This again shows similar pattern with that of extinction coefficient of figure4.10. The imaginary part of the dielectric constant ε_i increases with an increasing annealing temperature. ε_i generally decreases as photon energy increases.

The highest value of ε_i for as-deposited is 1.6 at photon energy of 1.5 eV and the ε_i range for post-deposition annealed samples is 1.5 to 2.28 at photon energy of 1.5 eV. The imaginary dielectric constant has its highest values for both as-deposited and annealed samples in the NIR-region which decreases towards the Vis-UV-regions of the electromagnetic spectrum. According to (Echendu et al, 2014) 'The observed values of ε_i suggest that devices fabricated at annealing temperature of 250 °C will display relatively improved and more stable capacitance and therefore will have longer response time in the infrared photon energy range compared to other annealing temperature'.

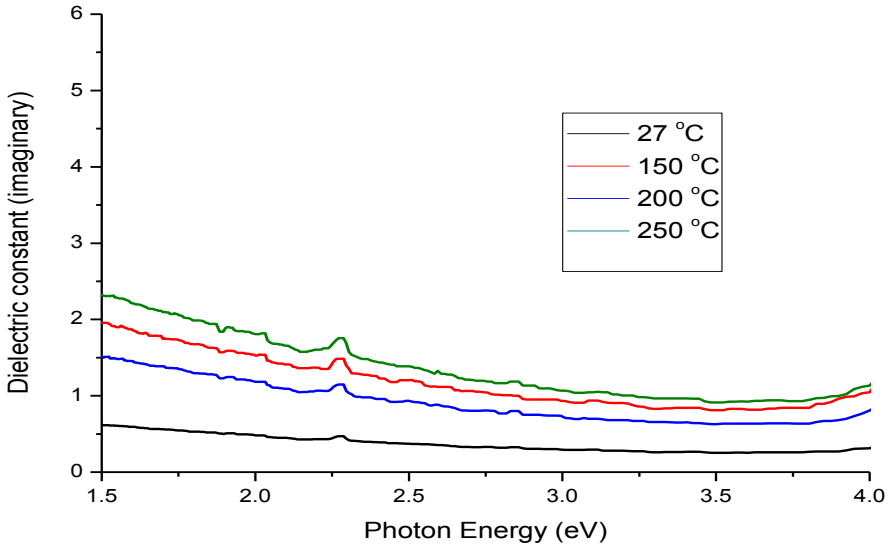

Figure 4.15 The spectral response of the imaginary dielectric constant ε_i versus photon energy for as-deposited and post-deposition annealed $CdAl_2SO_3$ thin films

4.5.2 Bandgap Energy (E_g)

The direct bandgap energy versus photon energy for as-deposited and post-deposition annealed $CdAl_2SO_3$ thin films is shown in figure 4.16. The graph shows $(\alpha h\nu)^2$ against $h\nu$ which is the famous Tauc method of determining energy bandgap. From the plot, the direct energy bandgap is estimated by extrapolating the straight line portion of the curve (after the absorption edge) to the point where $(\alpha h\nu)^2 = 0$.

The direct bandgap energy, $E_g$for as-deposited sample was estimated to be 4.1 eV, and the annealed materials have the bandgap in the range of 3.75 eV to 4.0 eV which is smaller compared to as deposited material. E_g decreases to 3.88 eV at annealing temperature of 150 °C, and then increases to 4.0 eV at annealing temperature of 200 °C, and again decreases to 3.75 eV at annealing temperature of 250 °C. Generally, bandgap energy decreases as annealing temperature increases. This could be caused by grain growth (Eya, *et al*., 2016). For bandgap energy, the optimal annealing temperature is 250 °C. The wide bandgap energy of $CdAl_2SO_3$ thin films can be aligned with materials with narrow bandgap such as SnS thin films reported by researchers to have E_g of the range 1.1 eV to 1.5 eV to achieve graded bandgap of high quality thin films material for solar energy conversion. The direct bandgap thin films could also be used to make optical devices such as LEDs and semiconductor lasers.

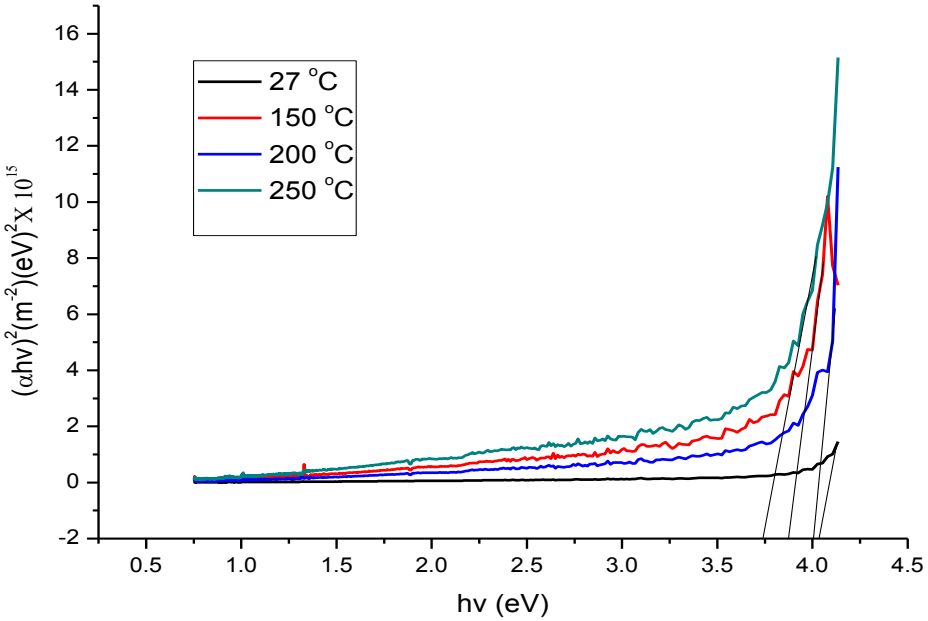

Fig. 4.16.The energy bandgap versus photon energy for as-deposited and post-deposition annealed *$CdAl_2SO_3$* thin films

CHAPTER 5

CONCLUSION AND RECOMMENDATIONS

5.1 Conclusion

The nanocrystallite $CdAl_2SO_3$ thin films were successfully prepared by chemical bath deposition (CBD) techniques. The films are white in colour and adhere firmly on the substrate. The optical properties of the films show that the films have high absorbance throughout the regions of the electromagnetic spectrum. The maximum value of absorbance is 99.5 % in the UV region and average of 95 % in the other regions of the spectrum. The film material generally has low transmittance across the spectrums from NIR-Vis to UV regions. The films have very low reflectance in as-deposited and annealed form across the UV-Vis-NIR regions, with the highest reflectance of about 1.5% in the visible region.The GIXRD patterns show that the quaternary cadmium aluminiumsulphite ($CdAl_2SO_3$) forms as a combination of monoclinic $CdSO_3$ and Al_2O_3.The direct bandgap energy ranges from 3.75 eV to 4.10 eV. Generally, the energy bandgap decreases as the annealing temperature increases. The thin films material can be used as a UV-shield owing to its ability to absorb very high ultra-violet radiation. The high absorption in the UV-Vis regions makes the thin films suitable for use as absorber layer in thin films solar cells. The poor reflectance of the films also indicates that it could be used as anti-reflection material. The relatively low refractive index shows that there will be minimal reflection loss when the material is used for thin films solar cells. The low dielectric constant makes the thin film material suitable for use as a photodedectors. The direct bandgap of the thin film material makes it applicable in optical devices such as LEDs and semiconductor lasers. The crystallite nanoscale size suggests the material could be used as quantum dots. These and other unexplored applications can be achieved from the $CdAl_2SO_3$ thin films.

5.2 Recommendations

Based on the challenges encountered in the cause of growing this thin films material, the following recommendations are proposed:

i. other methods of deposition such as: thermal evaporation, molecular beam epitaxy (MBE), chemical vapour deposition etc, should be explored and the results compared with the CBD method to know which method will give the best properties for the target application and

ii. conductive substrate such as fluorine doped tin oxide (FTO) or indium doped tin oxide (ITO) should be used for the films deposition to know how it will affect already established properties of the material.

5.3 Contribution to Knowledge

The cadmium aluminium sulphite, $CdAl_2SO_3$ is novel direct bandgap material with efficient optical properties for solar energy conversion. Owing to the high cost of silicon solar panel, $CdAl_2SO_3$ which is a relatively cheap material can be an alternative for solar panel fabrication.

REFERENCES

Amanullah, F.,Al-Shammari, S.,&Al-Dhafiri, A.(2005).Co-activation effect of chlorine on the physical properties of CdS thin films prepared by CBD technique for photovoltaic applications. *Journal of Physica Status Solidi (Applied Research)*, 202: 2474-2478.

Asim, J., Mohamed, S. W.,& Hammad, A. H.(2017). *Advance Deposition Techniques for Thin Film Coating*.

Bakke, J. R., Tangkanen,J. T., Hagglund,C., Pakkanen,T. A.,& Ben,S. F. (2012). Growth characteristics, material properties and optical properties of zinc oxysulphide films deposited by atomic layer deposition. *J. Vac. Sci. Technol*. A: Vac Surf Films 30, 01A135-1 - 01A135-8. doi.org/10.1116/1.3664758

Bhattacharya, S., Pramanick,P.,&Basa, P. K. (1987). Solution growth technique for deposition of cobalt solenoid thin films.*Thin Solid Films Lett*, 149, 181

Chao, G., Honglie,S.,& Sun,L. (2011). Preparation and properties of Zinc Blende and Orthorhombic SnS films by chemical bath deposition. *App. Surface Science*, 257. 6750-6756

Cheng, Q., Wang,D.,& Zhon,H. (2017). Electrodeposition of Zn(OS) (Zinc oxysulfide) thin films: exploiting its thermodynamic and kinetic processes with incorporation of tartaric acid. *J . Energy Chem.* https://doi.org/10.1016/j.jechem.2017.07.020(in press)

Choi, Young, Jim-Kung, Yoo., Boom,J., & Kin. Doughaun (1998). Properties of cadmium sulphide films deposited by chemical bath deposition with ultrasonication.*Sol. Ener. Mater*, 64 (1-3), 41

Chopra, K.L., &Das,S. R. (1983). Thin film solar cell.*Plenum Press New York.*

Chopra, K. L. (1969). Thin film phenomenon.*McGraw-Hill Book Company, New York* 96, 477

Coutts, T.J.,Ward, J.S., Young,D.L., Dessent,T. A.,& Noufi,R. (2001). The search for and potential impact of improved transparaent conducting oxides on thin film solar cells. *Technical digest of the 12th international photovoltaic science and engineering conference, Jeju Korea,* June 11-15.

Coutts, T. J., Emery,K.,& Ward,J. S. (2002). Modeled performance of polycrystalline thin film tandem cells.*Prog. Photovoltaic. Res. Appl.*, 10, 195-203

Cruz-Vazquez, A., Rocha-Alonzo,F., Burrel-Ibarra, S. E., Inoue,M., & Bernal,R. (2001). Fabrication and characterization of sulphur doped zinc oxide thin films.*Superficies Y Vacio*, 13, 89-91

Echendu, O. K. (2014). Thin film solar cells all-electrodeposited ZnS, CdS and CdTe materials. PhD. Thesis, *Sheffield Hallam University, United Kingdom.*

Echendu, O. K. , Weerasinghe,A. R., Disco,D. G., Fausi,F.& Dharmadas,I. M.(2013). Characterisation of n-type and p-type ZnS thin layers grown by electrochemical method. *J. Elect. Mater*: 42(11) 692-700

Echendu, O. K., Werta,S. Z., & Dejene,F. B.(2018). Effect of Cadmium precursor on the Physico-chemical properties of electrochemically grown CdS thin films for optoelectroniccs devices application: a comparative study. Journal of Material Science: *Materials in Electronics*,(2019) 30: 365-377.

Estrella, V., Nair,M. T. S., & Nair,P. K. (2003). Semiconducting Cu_3BiS_3 thin films formed by the solid state reaction of CuS and Bismuth thin films.*Semicond. Sci. Technol*, 18, 190

Eya, D. D. O. & Eze, F. C. (2011).Growth and characterization of chemically deposited deposied CdS-Cu_xS thin films. *Nig. Journal of Physics*; 22(**1**), 63-73.

Eya, D. D. O.,Eze, F.C., Echendu, O. K.& Mbamara, U. S. (2016).Synthesis and optical properties of chemically deposited cadmium sulphide thin films. *Nigerial Journal of Solar Energy*, Vol. 27.

Eze, F. C.,& Okeke,C. E. (1997). Chemical bath deposition of cobalt sulphide films preparation effects.*Material Chemistry and Physics*, 47, 31

Ezekoye, B.A,& Okeke,C.E. (2003). Solution growth and characterization of Cd1xZnxS alloy chalcogenide thin films for industrial and solar energy applications.*Nig. J. Solar Energy*, vol. 14, 82-89.

Estrella, V., Nair,M. T. S., & Nair,P. K. (2003). Semiconducting Cu3BiS3 thin films formed by the solid state reaction of CuS and Bismuth thin films.*Semicond. Sci. Technol*, 18, 190

Gunther, K. G. (1966). In the use of thin film in physical investigations.*J.C. Anderson (ed). Academic Press New York*

Heavens, O. S. (1970). Thin Film Physics.*Methuen and Co Ltd. London*

Henriquez, R., Froment,M., Riveros,G., Dalchiele,E. A., Gomez,H., Grez,P.,&Lincot,D. (2007). Electrodeposition of polyphasic films of zinc oxysulfide from DMSO onto n-Inp(100) and n-Inp(111) single crystals in the presence of zinc salt, thiourea and dissolved molecular oxygen.*J . Phys. Chem*, C111 (6017-6023)

Heujun. H, Guan,H.,& Lei, L. (2007). Sythesis of Cu_2FeSnS_4 thin films with Stannite and Wurtzite structure directly on glass substrate via the solvothermal method. *Journal of Materials Science Materials Electronics*, 28(11).doi: 10.1007/s 10854-017-6469-6

Hop, B. X., Trinh,H. V., Dat, K. Q., & Bao,P. Q. (2008). Growth of cadmium sulphide thin films by chemical bath deposition technique. *VNU journal of Science, Mathematic-Physics*,119-123

Huang, C.Y., Morse,S. M., Clark,A. H.& Kazmerski,L. I. (1982). Use of anion guage beam flux monitor for resistivity control in $CuInSe_2$grown by molecular beam epitaxy.*Solar Cells*, vol. 6 2, 191

Ibrahim, A. M. (1995). Optical properties of ternary AgSbS2 thin films. *J. Phys. Condense Matter* 7, 5931

Karlsson, P.G, Bolik,S., Richter, J.H., Mahrov,B., Johnansson,E.M.J., Blomquist,J., Uvdal,P., Rensmo,H., Sisghahn,H.& Sandell,A. (2004). Interface Properties of the Naon structural dye-sensitized solid

heterojunction Ti O2/RuI2(NCS)2/CUI.*Journal of Chemical Physics*, 120(23) 11224-1123

Khallaf, H., Chai, G., Lupan, O., Chow, L., Heinrich, H.,. Park, L. & Schult, A. (2009). Insitu boron doping of chemical-bath deposited CdS thin films. *Physica State Solda*, A206: 256–262.

Kijatkina, O., Mere, A., Mahrov,B., Dloczik, L.,& Krunks,M. (2003). $CuInS_2$ sprayed films on different metal Oxide underlayers.*Thin solid films*, 431, 105-109.

Kushwaha, V. S., Mehta,N.,& Kumar,A. (2005). High field conduction in amorphous thin films of Se70Te30-xCdx in dark and in the presence of light.*Indian Journal of Pure and Applied Physics*, vol. 23, 636

Lee, J. H., Song,W., Yi,J.,&Yoo, J. (2003). Characteristics of CdZnS thin film doped by thermal diffusion of vacuum evaporated indium films.*Solar Energy Mater*, 75, 227

Lei, M., Yongfeng,L., Bin,Y., Zhan-Hui,D., Gang,Y., Rui-Jian,L., Rui,D.,& Lei,L. (2015). Mechanism of effect of intrinsic defects on electrical and optical properties of Cu_2CdSnS_4: an experimental and first-principles study. *Journal of Physics*, Volume 48, Number 44

Lothian, G.F. (1958). Absorption Spectrophotometry. *2nd edn, Hisher and Watts Ltd London*, 19, 20.

Mahrov, B., Boschloo,G., Hyfeldt,A., Siegbahn,H.,&Rensmo,H. (2004). Photoelectron spectroscopy studies of Ru(dcbpyH2)2(NCS)2/CuI and Ru(dcbpyH2)2/CuSCN interfaces for solar cell applications.*Journal of Physical Chemistry B*, 108 (31), 11604-11610.

Maissel, L. I. (1966). In physics of thin films.*G. Hasi and R.E. Tun (eds) vol. 3, Academic Press Inc. New York*, 61

Maissel, L. I., & Glang,R. (1970). Handbook of thin film technology. *McGraw Hill, New York.*

Mosiori, C. (2012). Electrical And Optical Characterization Of $Cd_xZn_{1-x}S$ And PbS Thin Films for Photovoltaic Applications. *MSc. Thesis, Kenyatta University, Kenya.*

Myers, D., Emery,K.,& Kurtz,S. (2002). Proposed reference spectral irradiance standards to improve concentring photovoltaic system design and performance evaluation concentrator cells.*29th IEEE PVSC New Orleans*

Nair, P. K., Nair,M.T. S.,& Campos,J. (1987). Photocurrent response in chemically deposited CdS thin films.*Sol. Ener. Mater*, 15, 153

Ndukwe, I. C. (1992). The growth and characterisation of thin films by solution growth technique and their applications. *Ph.D Thesis, University of Nigeria Nsukka.*

Okoli, D. N., Ekpunobi,A. J., &Okeke,C. E. (2006). Optical Properties of AgAlS2 Thin Films Prepared by Chemical Bath Deposition Technique.*Academic open Internet Journal*, Vol. 18, part 5.

Onyegbule, L. O. (2015). Chemical bath deposition and characterisation of SnS and SnS-Cu_xS. *MSc. Thesis, Federal University of Technology Owerri.*

Ortega-Lopez, M., Vigil-Galan, O., Cruz-Gandarilla,F., &Solarza-Feria, O. (2003). Preparation of $AgInS_2$ chalcopyrite thin films by chemical spray pyrolysis.*Materials Research Bulletin*, 38, 55-61

Pankove, J.I (1971). Optical processes in semiconductors. *Prentice-Hall, New York.*

Pawar, S. H., Tamhankar, S. P.,& Lokhande,C. D. (1986). Studies on electrochemical photovoltaic cells formed with thin film BiCdS4 photoelectrodes.*Sol. Ener. Mater*, 14, 71-74

Pentia, E., Draghici,V., Sarua,G., Mereu,B., Pintilie,L., Sava,F.,& M. Popescu,F. (2004). Structural electrical and photoelectrical properties of CdxPb1-xS thin film prepared by chemical bath deposition.*J. Electrochem. Soc. Vol.* 151 (11) 729-733

Polat, I., Aksu,S., Itunbas,M. A., Yilmaz,S.,& Bacaksiz,E. (2011). The influence of diffusion temperature on the structural, optical and magnetic properties of manganese-doped zinc oxysulfide thin films.*J. Solid State Chem.* 184 (2683-2689)

Quimby, R. S.(2006). Photonics and lasers: An Introduction*(Hoboken, NJ: Wiley*, 2006), P.259

Rai, J. P. (1993). Electrosynthesis of zinc selenide and thallium containing zinc selenide thin film and their characterization.*Solar Ener. Mater*.

Renishaw plc (2001-2019). https://www.renishaw.com/en/raman-bands explained-25808.

Shadia, K., Mangalaraj, D., Narayandass, K., Hong, B., Roh, Y., Park, C. and Junsin, Y. (2008). Argon and nitrogen implantation effects on the structural and optical properties of vacuum evaporated cadmium sulphide thin films.

Scriven, L.E., Brinker,C. J., Clark,D. E.,& Urich,D. R. (1988). Better ceramics through chemistry II. Mater. Res. Soc. Symp. Proc. vol. 121, *Material Research Society* mttsburg 717

Uhuegbu, C. C., (2011). Spectral Selective Properties and Possible Applications of Iron Zinc Sulphide Ternary Thin Film. *Journal of Basic and Applied Scientific Research*, 1(4)307-311.

Woon-Jo, Jeong,& Park Cye-Cheon (2003). Structural and electrical properties of CuGaS2 thin films by electron beam evaporation. *Solar Energy Materials and Solar Cells*,75, 93-100

Wooten &Fredrick. (1972). Optical properties of solids.*Academic Press. New York*

Xie, .M, Daming,Z., Ming,Z., Zhuang,Z., Liangqi, O., Xiaolong,L.,&Song,S. (2013). Preparation and characterization of Cu_2ZnSnS_4 thin films and solar cells fabrication from quaternary Cu-Zn-Sn-S target. *International Journal of Photoenergy*, Article ID 929454, 9 pages.http://dx.doi.org/10.1155/2013/929454

Xiaohui, M., Ruizhi,C., &Wenjuan,C. (2017). Synthasis and Characterization of Cu_2FeSnS_4 thin films prepared by electrochemical deposition. *Materials Letters* 193. doi. 10.1016/j.matlet.2017.01.099